Transportation Research Part C 152 (2023) 104159

Contents lists available at ScienceDirect

Transportation Research Part C

journal homepage: www.elsevier.com/locate/trc

Dynamic ride-sourcing systems for city-scale networks, Part II: Proactive vehicle repositioning

Amir Hosein Valadkhani, Mohsen Ramezani *

The University of Sydney, School of Civil Engineering, Sydney, Australia

ARTICLE INFO

Keywords:
On-demand mobility
Transportation network company (TNC)
E-hailing
Proactive control
Rebalancing
Supply and demand matching

ABSTRACT

The emergence of ride-sourcing systems has unprecedentedly changed the market for on-demand mobility services. The service quality of the ride-sourcing systems and their effects on transportation networks rely on effective matching and *redistributing of idle vehicles*. In Part I, we introduced a vehicle–passenger matching method that jointly determines the maximum matching distance and matching intervals to minimize passengers waiting time. Moreover, a non-equilibrium macroscopic model is developed to predict the evolution of the ride-sourcing system states. In this paper, we propose a control method to transfer idle vehicles to balance the passengers' demand and supply of ride-sourcing vehicles by repositioning the idle vehicles in locations where there is a higher possibility of faster pickups of new passengers. This paper develops a Nonlinear Model Predictive Controller (NMPC) that proactively transfers idle vehicles based on the predicted future state of the ride-sourcing system using the non-equilibrium model developed in Part I paper. The proposed NMPC implements an optimum rolling horizon strategy that solves a constrained optimization problem at each transferring sample time. The proposed method considers the effect of network congestion and impatient passengers and drivers. We show that the proactiveness of the NMPC incentivizes the drivers to follow the transferring commands instead of random cruising during idle periods. In microsimulation experiments, the designed controller improves the performance of the ride-sourcing system by reducing passengers' average unassigned time (-20.4%) and waiting times (-12.4%), vehicles' average waiting times (-8.8%), the fleet size (-18.6%), and increasing the number of the served trip requests (9.7%).

1. Introduction

The emergence of ride-sourcing systems with internet-based platforms has introduced a popular transportation mode in recent years. There has been a continuing debate/research about the effect of dispatching methods of ride-sourcing systems on network congestion, deadheading time of the vehicles, and waiting time of the passengers. The dispatching method is a critical component of the ride-sourcing systems that assigns idle vehicles to waiting passengers (i.e., travel requests). Manipulation of idle vehicle positions is a method to complement the dispatching method. In this study, we propose a dynamic transferring method for repositioning idle vehicles to locations with a higher probability of being assigned to new incoming passengers. A Nonlinear Model Predictive Controller (NMPC) is designed as a proactive transferring method to reduce (i) passengers' unassigned and waiting times, (ii) vehicles' waiting times, and (iii) guided vacant cruising distances. We use the developed macroscopic non-equilibrium model introduced in Part I paper to design the controller.

* Corresponding author.
E-mail address: mohsen.ramezani@sydney.edu.au (M. Ramezani).

https://doi.org/10.1016/j.trc.2023.104159
Received 23 December 2022; Received in revised form 27 April 2023; Accepted 29 April 2023
Available online 15 May 2023

Ride-sourcing systems have been studied from different perspectives, such as pricing of the service (Zha et al., 2018a,b; Nourinejad and Ramezani, 2019; Battifarano and Qian, 2019; Zuniga-Garcia et al., 2020; Jiao and Ramezani, 2022), demand or supply estimation (Wu et al., 2018; Ke et al., 2017, 2018), fleet size management (Vazifeh et al., 2018), and vehicle–passenger matching method (Maciejewski et al., 2016; Yang et al., 2020; Chen et al., 2021). Interested readers are referred to Wang and Yang (2019) and Narayanan et al. (2020) for detailed reviews on ride-sourcing systems.

A group of articles in the literature study the repositioning of idle vehicles without considering the dynamic evolution of the system (i.e., reactive repositioning) or between specific stations/nodes. For example Pavone et al. (2012), Zhang and Pavone (2016), Braverman et al. (2019) propose repositioning methods by assuming stationary conditions. Sayarshad and Chow (2017) studies a non-myopic policy for idle vehicle repositioning between a set of stations/nodes using queueing delay as an approximation of the conditional expected cost. In Alonso-Mora et al. (2017), a scalable method is suggested for relocating idle vehicles to regions with high instantaneous demand. A rebalancing method is studied in Ramezani and Nourinejad (2018) for a street-hailing taxi system based on macroscopic fundamental diagrams (MFDs). Yang and Ramezani (2023) proposes a learning method for real-time repositioning in e-hailing services. Demand forecasting is incorporated into the paradigm of repositioning the on-demand mobility systems in Dandl et al. (2019). One-way vehicle relocation among the fixed nodes is studied in Illgen and Höck (2019), Nourinejad et al. (2015).

Reactive repositioning of idle vehicles does not consider the intertwined effects of transferring the idle vehicles at the current time, the future state of vehicle–passenger matchings, and vehicle and waiting passengers arrivals. Reactive transferring may lead to side effects such as increasing the deadheading time and dead-mileage of idle vehicles. Moreover, relocating idle vehicles between a small number of nodes/stations lacks scalability for network-wide ride-sourcing systems. To fill the gap in the literature, we develop a proactive repositioning method based on NMPC for ride-sourcing systems that is beneficial for drivers to follow the repositioning recommendations of the system to reduce the waiting time of the passengers.

In Part I, an adaptive spatio-temporal matching method is proposed to dynamically determine the optimum values of maximum matching distance (to discard long-distance vehicle–passenger matchings) and the next matching instance (to establish a time-varying matching frequency). The developed method considers the joint effects of matching intervals and maximum matching distances to minimize passengers' waiting time and to avoid unnecessarily long-distance matchings. In this paper, we focus on the repositioning of idle vehicles to curb the possible mismatch between supply and demand in the system. To this end, we propose an NMPC as a systematic proactive repositioning method for balancing idle vehicles and waiting passengers in a network that is partitioned into a number of regions. This study develops a real-time scalable repositioning method that considers the dynamic evolution of the ride-sourcing system's state (e.g., prediction of the number of idle/ dispatched/ occupied/ transferred vehicles, waiting/ assigned/ on-board passengers) and vehicle–passenger matching rates in each region based on the developed model in Part I.

The NMPC provides the number of vehicles to reposition between every two regions. This information is translated to individual vehicles by solving heuristically an integer optimization problem that is equivalent to finding a subset of a maximum matching of a bipartite graph. In this problem, each side of the bipartite graph is partitioned into a set of disjoint subsets (i.e., supply and demand). A subset is defined as a *supply* region if there is an excess number of idle vehicles to be transferred from, and is defined as a *demand* region if there is a shortage of idle vehicles to be the destination of transferring vehicles. Nodes in supply regions are the current location of idle vehicles (i.e., origins of transferring). Nodes in the demand regions are candidate locations (i.e., destinations of transferring) that are chosen randomly around the geometric center of available waiting passengers of the demand region. The weights of the graph are negative of the shortest travel time between the idle vehicles in supply regions and the candidate locations in the demand regions. By solving subsets of maximum matching of the bipartite graph, the repositioning controller determines pairs of origins and destinations for transferring idle vehicles at each transferring time.

The proposed method considers the variation of demand (i.e., passengers' trip requests) and supply (i.e., ride-sourcing vehicles) as well as the effect of estimated network congestion, impatient drivers, and impatient passengers. We show that the proactiveness of the NMPC reduces the dispatching distances of the vehicles that are transferred to the recommended locations. The proposed method lowers passengers' and vehicles' total delay, increases the number of the served passengers' trip requests, and reduces the required fleet size.

This article is organized as follows. Section 2 elaborates the framework of the dynamic vehicle repositioning system and introduces the mathematical formulation of the transferring system in a state–space form. In Section 3, we propose a nonlinear model predictive controller (NMPC) that is built upon solving a rolling-horizon constrained optimization problem. Further, we discuss the estimation of the endogenous inputs for improving the ride-sourcing system's controllability. In Section 4, we present the microsimulation setup, a reactive controller, and the results of the transferring method on a traffic microsimulation model. The paper is summarized and the future research directions are discussed in Section 5.

2. Vehicle repositioning framework and formulation

2.1. Framework

The developed ride-sourcing system has two main components: dispatching (introduced in Part I paper) and transfer subsystems. We consider ride-sourcing vehicles cannot be street-hailed and should be dispatched to the waiting passengers for pickup. The dispatching subsystem assigns waiting passengers to vacant vehicles (i.e., idle and transferred vehicles) in each matching instance. The transfer subsystem uses the developed model in Part I to predict the evolution of the idle, transferred, dispatched, and occupied

vehicles as well as waiting and assigned passengers in different regions of the network. It sends the idle vehicles to the regions with an excess number of waiting passengers to balance the demand of passengers' travel requests with idle vehicles in each region. We consider idle vehicles cruise around (randomly) before being matched or transferred by the ride-sourcing system. In each *transfer time instance* (i.e., time instances when the transfer subsystem is triggered), the transfer subsystem selects a part of idle vehicles and transfers them to the regions with a high possibility of finding passengers in the subsequent matching instances (i.e., near future). Selected idle vehicles follow the routing recommendation of the ride-sourcing system.

The transfer subsystem determines the inter-regional movements of a set of idle ride-sourcing vehicles based on real-time information of the network and the developed mathematical model. The transfer subsystem, in each transferring time instance, obtains the number of (i) idle vehicles in every region, (ii) transfer, dispatch, and occupied vehicles in Region i with destinations in Region j, and (iii) waiting and assigned passengers in Region i with destinations in Region j. In addition, the transfer subsystem at each transfer time instance requires an estimation of the rate of (i) incoming idle vehicles in each region and (ii) new waiting passengers in Region i with destinations in Region j.

The transfer subsystem utilizes the above information periodically to predict the macroscopic behavior of the network (i.e., the evolution of different states of the ride-sourcing system). The predictions are used to determine the rate of transferring the idle vehicles to the regions with a higher possibility of matching with the waiting passengers.

2.2. Model formulation

In this part, the summary of the model developed in Part I is briefly re-introduced. In the second part of this section, the state–space representation of the model utilized to design the repositioning controller is formulated.

2.2.1. Summary of the model

This subsection briefly summarizes the developed macroscopic ride-sourcing model in Part I. The model utilizes the Cobb–Douglas meeting function and Macroscopic Fundamental Diagram (MFD) (Ramezani and Nourinejad, 2018) to represent the evolution of idle, transferred, dispatched, and occupied vehicles as well as waiting and assigned passengers in each region of the network. In Eqs. (1) to (11), subscript ij denotes from current Region i to final destination j. The set of network regions is denoted by $\mathbb{R}$ and $\mathbb{U}_i$ is the set of regions in the direct vicinity of Region i.

Evolution of the occupied vehicles, c_{ii}^{O} and c_{ij}^{O}, are formulated in Eqs. (1) and (2). The number of dispatched vehicles that become occupied at time t is denoted by $b_{ii}(t)$ and $b_{ij}(t)$.

$$\frac{\mathrm{d}c_{ii}^{\mathrm{O}}(t)}{\mathrm{d}t} = b_{ii}(t) + \sum_{j\in\mathbb{U}_i} M_{ji}^{\mathrm{O}}(t) - M_{ii}^{\mathrm{O}}(t) \qquad \forall i \in \mathbb{R}, \tag{1}$$

$$\frac{\mathrm{d}c_{ij}^{\mathrm{O}}(t)}{\mathrm{d}t} = b_{ij}(t) - M_{ij}^{\mathrm{O}}(t) \qquad \forall i \in \mathbb{R} \ \text{ and } \ j \in \mathbb{U}_i. \tag{2}$$

Eqs. (3) and (4) show the conservation equations of dispatched vehicles, $c_{ii}^{\mathrm{D}}(t)$ and $c_{ij}^{\mathrm{D}}(t)$, where $W_{ii}^{\mathrm{I\text{-}D}}(t)$ and $W_{ij}^{\mathrm{I\text{-}D}}(t)$ are the rate at which idle vehicles become dispatched at time t. The rate transferred vehicles become dispatched are denoted by $W_{ii}^{\mathrm{T\text{-}D}}(t)$ and $W_{ij}^{\mathrm{T\text{-}D}}(t)$. Inter-regional flow of dispatched vehicles is denoted by $M_{ij}^{\mathrm{D}}(t)$. Furthermore, $R_{ii}^{\mathrm{D}}(t)$ and $R_{ij}^{\mathrm{D}}(t)$ are cancellation rates of dispatched vehicles by impatient passengers at time t.

$$\frac{\mathrm{d}c_{ii}^{\mathrm{D}}(t)}{\mathrm{d}t} = W_{ii}^{\mathrm{I\text{-}D}}(t) + W_{ii}^{\mathrm{T\text{-}D}}(t) + \sum_{j\in\mathbb{U}_i} M_{ji}^{\mathrm{D}}(t) - b_i(t) - R_{ii}^{\mathrm{D}}(t) \qquad \forall i \in \mathbb{R}, \tag{3}$$

$$\frac{\mathrm{d}c_{ij}^{\mathrm{D}}(t)}{\mathrm{d}t} = W_{ij}^{\mathrm{I\text{-}D}}(t) + W_{ij}^{\mathrm{T\text{-}D}}(t) - M_{ij}^{\mathrm{D}}(t) - R_{ij}^{\mathrm{D}}(t) \qquad \forall i \in \mathbb{R} \ \text{ and } \ j \in \mathbb{U}_i. \tag{4}$$

The change in the number of transferred vehicles at time t is determined by Eqs. (5) and (6), where $M_{ii}^{\mathrm{T}}(t)$ and $M_{ij}^{\mathrm{T}}(t)$ denote internal and inter-regional flows of transferred vehicles, respectively. $W_{ij}^{\mathrm{I\text{-}T}}(t)$ is the rate at which idle vehicles are transferred by the transfer controller.

$$\frac{\mathrm{d}c_{ii}^{\mathrm{T}}(t)}{\mathrm{d}t} = \sum_{j\in\mathbb{U}_i} M_{ji}^{\mathrm{T}}(t) - M_{ii}^{\mathrm{T}}(t) - W_{ii}^{\mathrm{T\text{-}D}}(t) \qquad \forall i \in \mathbb{R}, \tag{5}$$

$$\frac{\mathrm{d}c_{ij}^{\mathrm{T}}(t)}{\mathrm{d}t} = W_{ij}^{\mathrm{I\text{-}T}}(t) - M_{ij}^{\mathrm{T}}(t) - W_{ij}^{\mathrm{T\text{-}D}}(t) \qquad \forall i \in \mathbb{R} \ \text{ and } \ j \in \mathbb{U}_i. \tag{6}$$

The change in the number of idle vehicles in each region, $c_i^{\mathrm{I}}(t)$, can be obtained by Eq. (7). The exogenous arrival and leaving rates of idle vehicles are denoted by $q_i^{c^+}(t)$ and $q_i^{c^-}(t)$, respectively. $w_i^{\mathrm{I}}(t)$ is the rate of idle vehicles that are close to the boundary of the regions and might leave their current region because of random cruising behavior of idle vehicles.

$$\frac{\mathrm{d}c_i^{\mathrm{I}}(t)}{\mathrm{d}t} = q_i^{c^+}(t) + M_{ii}^{\mathrm{O}}(t) + M_{ii}^{\mathrm{T}}(t) - q_i^{c^-}(t) + \sum_{j\in\{\mathbb{U}_i,i\}} R_{ij}^{\mathrm{D}}(t) - \sum_{j\in\{\mathbb{U}_i,i\}} W_{ij}^{\mathrm{I\text{-}D}}(t) - \sum_{j\in\mathbb{U}_i} W_{ij}^{\mathrm{I\text{-}T}}(t) + w_i^{\mathrm{I}}(t) \qquad \forall i \in \mathbb{R}. \tag{7}$$

The evolution of the numbers of waiting passengers are:

$$\frac{\mathrm{d}p_{ii}^{\mathrm{W}}(t)}{\mathrm{d}t} = q_{ii}^{p^{W+}}(t) - q_{ii}^{p^{W-}}(t) - W_{ii}^{\text{W-A}}(t) \qquad \forall i \in \mathbb{R}, \tag{8}$$

$$\frac{\mathrm{d}p_{ij}^{\mathrm{W}}(t)}{\mathrm{d}t} = q_{ij}^{p^{W+}}(t) - q_{ij}^{p^{W-}}(t) - W_{ij}^{\text{W-A}}(t) \qquad \forall i \in \mathbb{R} \ \text{ and } \ j \in \mathbb{U}_i, \tag{9}$$

where $W_{ii}^{\text{W-A}}(t)$ and $W_{ij}^{\text{W-A}}(t)$ are the rates waiting passengers become assigned at time t. The exogenous arrival rates of waiting passengers are $q_{ii}^{p^{W+}}(t)$ and $q_{ij}^{p^{W+}}(t)$. $q_{ij}^{p^{W-}}(t)$ and $q_{ij}^{p^{W-}}(t)$ denote the exogenous leaving rates of waiting passengers.

The number of assigned passengers can be tracked by Eqs. (10) and (11). In these equations, $q_{ii}^{p^{A-}}(t)$ and $q_{ij}^{p^{A-}}(t)$ are the rates of order cancellation of impatient waiting passengers.

$$\frac{\mathrm{d}p_{ii}^{\mathrm{A}}(t)}{\mathrm{d}t} = W_{ii}^{\text{W-A}}(t) - q_{ii}^{p^{A-}}(t) - b_{ii}(t) \qquad \forall i \in \mathbb{R}, \tag{10}$$

$$\frac{\mathrm{d}p_{ij}^{\mathrm{A}}(t)}{\mathrm{d}t} = W_{ij}^{\text{W-A}}(t) - q_{ij}^{p^{A-}}(t) - b_{ij}(t) \qquad \forall i \in \mathbb{R} \ \text{ and } \ j \in \mathbb{U}_i. \tag{11}$$

2.2.2. State–space formulation

In this subsection, we introduce the mathematical formulation of the model in a standard state–space form to design the transfer controller. The controller for repositioning the vehicles is designed based on the developed model in Part I that assumes the network is partitioned into a set of regions denoted by $\mathbb{R}$. In the developed model, there are four groups of vehicles (i.e., idle, transferred, dispatched, and occupied) and three groups of passengers (i.e., waiting, assigned, and on-board). The state variables that correspond to each group of vehicles and passengers are:

$$\boldsymbol{X}(t) = [\boldsymbol{C}^{\mathrm{I}}(t), \boldsymbol{C}^{\mathrm{T}}(t), \boldsymbol{C}^{\mathrm{D}}(t), \boldsymbol{C}^{\mathrm{O}}(t), \boldsymbol{P}^{\mathrm{W}}(t), \boldsymbol{P}^{\mathrm{A}}(t)]^{\top}, \ \boldsymbol{X}(t) \subset \mathcal{R}^{6N+5\sum_{i=1}^{N}\|\mathbb{U}_i\|} \tag{12}$$

where $\top$ is the transpose operator and $\mathcal{R}$ denotes the set of real numbers. $\mathbb{U}_i$ is the set of the regions directly connected to Region i and $\|\mathbb{U}_i\|$ is the cardinality of $\mathbb{U}_i$. The number of regions in the network in denoted by N. Each state of the ride-sourcing system can be decomposed by row-wise concatenation of submatrices such as $c_{ik_i}^{\mathrm{T}}(t)$, $c_{ik_i}^{\mathrm{D}}(t)$, $c_{ik_i}^{\mathrm{O}}(t)$, $c_{ik_i}^{\mathrm{D}}(t)$, $p_{ik_i}^{\mathrm{W}}(t)$, and $p_{ik_i}^{\mathrm{A}}(t) \subset \mathcal{R}^{\left(1+\|\mathbb{U}_i\|\right)\times 1}$, where $\mathcal{R}^{\left(1+\|\mathbb{U}_i\|\right)\times 1}$ denotes the set of real-valued matrices with the size of $\left(1+\|\mathbb{U}_i\|\right)\times 1$. The decomposition of each state is:

$$\boldsymbol{C}^{\mathrm{T}}(t) = \begin{bmatrix} \left[c_{1k_1}^{\mathrm{T}}(t)\right]_{\left(1+\|\mathbb{U}_1\|\right)\times 1} \\ \vdots \\ \left[c_{ik_i}^{\mathrm{T}}(t)\right]_{\left(1+\|\mathbb{U}_i\|\right)\times 1} \\ \vdots \\ \left[c_{Nk_N}^{\mathrm{T}}(t)\right]_{\left(1+\|\mathbb{U}_N\|\right)\times 1} \end{bmatrix}, \boldsymbol{C}^{\mathrm{D}}(t) = \begin{bmatrix} \left[c_{1k_1}^{\mathrm{D}}(t)\right]_{\left(1+\|\mathbb{U}_1\|\right)\times 1} \\ \vdots \\ \left[c_{ik_i}^{\mathrm{D}}(t)\right]_{\left(1+\|\mathbb{U}_i\|\right)\times 1} \\ \vdots \\ \left[c_{Nk_N}^{\mathrm{D}}(t)\right]_{\left(1+\|\mathbb{U}_N\|\right)\times 1} \end{bmatrix}, \boldsymbol{C}^{\mathrm{O}}(t) = \begin{bmatrix} \left[c_{1k_1}^{\mathrm{O}}(t)\right]_{\left(1+\|\mathbb{U}_1\|\right)\times 1} \\ \vdots \\ \left[c_{ik_i}^{\mathrm{O}}(t)\right]_{\left(1+\|\mathbb{U}_i\|\right)\times 1} \\ \vdots \\ \left[c_{Nk_N}^{\mathrm{O}}(t)\right]_{\left(1+\|\mathbb{U}_N\|\right)\times 1} \end{bmatrix},$$

$$\boldsymbol{C}^{\mathrm{I}}(t) = \begin{bmatrix} c_1^{\mathrm{I}}(t) \\ \vdots \\ c_i^{\mathrm{I}}(t) \\ \\ \vdots \\ c_N^{\mathrm{I}}(t) \end{bmatrix}, \boldsymbol{P}^{\mathrm{W}}(t) = \begin{bmatrix} \left[p_{1k_1}^{\mathrm{W}}(t)\right]_{\left(1+\|\mathbb{U}_1\|\right)\times 1} \\ \vdots \\ \left[p_{ik_i}^{\mathrm{W}}(t)\right]_{\left(1+\|\mathbb{U}_i\|\right)\times 1} \\ \vdots \\ \left[p_{Nk_N}^{\mathrm{W}}(t)\right]_{\left(1+\|\mathbb{U}_N\|\right)\times 1} \end{bmatrix}, \boldsymbol{P}^{\mathrm{A}}(t) = \begin{bmatrix} \left[p_{1k_1}^{\mathrm{A}}(t)\right]_{\left(1+\|\mathbb{U}_1\|\right)\times 1} \\ \vdots \\ \left[p_{ik_i}^{\mathrm{A}}(t)\right]_{\left(1+\|\mathbb{U}_i\|\right)\times 1} \\ \vdots \\ \left[p_{Nk_N}^{\mathrm{A}}(t)\right]_{\left(1+\|\mathbb{U}_N\|\right)\times 1} \end{bmatrix}, \tag{13}$$

where $k_i \in \{\mathbb{U}_i, i\}$. $c_{ik_i}^{\mathrm{T}}(t)$, $c_{ik_i}^{\mathrm{D}}(t)$, $c_{ik_i}^{\mathrm{O}}(t)$, $p_{ik_i}^{\mathrm{W}}(t)$, and $p_{ik_i}^{\mathrm{A}}(t)$ are the numbers of the transfer vehicles, dispatched vehicles, occupied vehicles, waiting passengers, and assigned passengers in Region i with final destinations in Region k_i at time t. $c_i^{\mathrm{I}}(t)$ denotes the number of idle vehicles in Region i at time t. We do not track the number of on-board passengers as a state variable because the number of on-board passengers and occupied vehicles are equal at all times.

To obtain the nonlinear state–space form of the model for designing the controller, we categorize the inputs of the ride-sourcing system and the transfer controller into four types:

(i) *Exogenous inputs*: the arrival rate of new ride-sourcing vehicles (i.e., drivers who start providing rides), $q_i^{c^+}(t)$, and the rate of idle vehicles leaving the ride-sourcing system (i.e., drivers who finish providing rides), $q_i^{c^-}(t)$, are the external inputs of idle vehicles in Region i. The external demand of waiting passengers in Region i with destinations in Region j, $q_{ij}^{p^{W+}}(t)$, is the rate passengers enter the ride-sourcing system (see Eqs. (7) to (9)). The vector of the exogenous inputs is:

$$\begin{aligned} &\boldsymbol{U}^{\mathrm{ex}}(t) = [\boldsymbol{Q}^{c^+}(t), \boldsymbol{Q}^{c^-}(t), \boldsymbol{Q}^{p^{W+}}(t)] \qquad \boldsymbol{U}^{\mathrm{ex}}(t) \subset \mathcal{R}^{3N+\sum_{i=1}^{N}\|\mathbb{U}_i\|}, \\ &\boldsymbol{Q}^{c^+}(t) = [q_1^{c^+}(t), \ldots, q_i^{c^+}(t), \ldots, q_N^{c^+}(t)], \\ &\boldsymbol{Q}^{c^-}(t) = [q_1^{c^-}(t), \ldots, q_i^{c^-}(t), \ldots, q_N^{c^-}(t)], \\ &\boldsymbol{Q}^{p^{W+}}(t) = \left[\left[q_{1k_1}^{p^{W+}}(t)\right]_{\left(1+\|\mathbb{U}_1\|\right)\times 1}, \ldots, \left[q_{ik_i}^{p^{W+}}(t)\right]_{\left(1+\|\mathbb{U}_i\|\right)\times 1}, \ldots, \left[q_{Nk_N}^{p^{W+}}(t)\right]_{\left(1+\|\mathbb{U}_N\|\right)\times 1}\right]. \end{aligned} \tag{14}$$

(ii) *Endogenous inputs*: these inputs are influenced by the dispatching subsystem. They are the results of the proposed adaptive spatio-temporal matching method in Part I. $W_{ij}^{\text{I-D}}(t)$, $W_{ij}^{\text{T-D}}(t)$, and $W_{ij}^{\text{W-A}}(t)$, $\forall i$ and $j \in \mathbb{R}$, denote the endogenous inputs. $W_{ij}^{\text{I-D}}(t)$ and $W_{ij}^{\text{T-D}}(t)$ are the rates of idle and transferred vehicles in Region i that are dispatched to Region j, respectively. The rate of waiting passengers in Region i with destinations in Region j that are assigned to the vehicles by the matching method is denoted by $W_{ij}^{\text{W-A}}(t)$ (see Eqs. (3) to (11)). The endogenous inputs are vectorized as:

$$\begin{aligned}
&\boldsymbol{U}^{\text{en}}(t) = \left[\boldsymbol{W}^{\text{I-D}}(t), \boldsymbol{W}^{\text{T-D}}(t), \boldsymbol{W}^{\text{W-A}}(t)\right] \qquad \boldsymbol{U}^{\text{en}}(t) \subset \mathcal{R}^{3(N+\sum_{i=1}^{N}\|\mathbb{U}_i\|)},\\
&\boldsymbol{W}^{\text{I-D}}(t) = \left[\left[W_{1k_1}^{\text{I-D}}(t)\right]_{\left(1+\|\mathbb{U}_1\|\right)\times 1}, \dots, \left[W_{ik_i}^{\text{I-D}}(t)\right]_{\left(1+\|\mathbb{U}_i\|\right)\times 1}, \dots, \left[W_{Nk_N}^{\text{I-D}}(t)\right]_{\left(1+\|\mathbb{U}_N\|\right)\times 1}\right],\\
&\boldsymbol{W}^{\text{T-D}}(t) = \left[\left[W_{1k_1}^{\text{T-D}}(t)\right]_{\left(1+\|\mathbb{U}_1\|\right)\times 1}, \dots, \left[W_{ik_i}^{\text{T-D}}(t)\right]_{\left(1+\|\mathbb{U}_i\|\right)\times 1}, \dots, \left[W_{Nk_N}^{\text{T-D}}(t)\right]_{\left(1+\|\mathbb{U}_N\|\right)\times 1}\right],\\
&\boldsymbol{W}^{\text{W-A}}(t) = \left[\left[W_{1k_1}^{\text{W-A}}(t)\right]_{\left(1+\|\mathbb{U}_1\|\right)\times 1}, \dots, \left[W_{ik_i}^{\text{W-A}}(t)\right]_{\left(1+\|\mathbb{U}_i\|\right)\times 1}, \dots, \left[W_{Nk_N}^{\text{W-A}}(t)\right]_{\left(1+\|\mathbb{U}_N\|\right)\times 1}\right].
\end{aligned} \tag{15}$$

The dynamics of the endogenous inputs and how they react to the vehicle repositioning are crucial for determining the optimum rate of idle vehicles being transferred. These inputs are considered known in Part I that reduce the controllability of the model. In Section 3.2, estimations of the predicted values of the endogenous inputs are presented to capture the dependencies of these inputs and the model.

(iii) *Control inputs*: these inputs are manipulated by the transfer subsystem for dynamically rebalancing the number of idle vehicles in each region. $W_{ij}^{\text{I-T}}(t)$, $\forall i \in \mathbb{R}$ and $j \in \mathbb{U}_i$, is the control input (see Eqs. (5) and (6)). This is the rate of idle vehicles in Region i being advised to transfer to Region j by the controller. The control inputs, $\boldsymbol{U}^{\text{co}}(t) \subset \mathcal{R}^{\sum_{i=1}^{N}\|\mathbb{U}_i\|}$, are:

$$\boldsymbol{U}^{\text{co}}(t) = \left[\left[W_{1k_1}^{\text{I-T}}(t)\right]_{\|\mathbb{U}_1\|\times 1}, \dots, \left[W_{ik_i}^{\text{I-T}}(t)\right]_{\|\mathbb{U}_i\|\times 1}, \dots, \left[W_{Nk_N}^{\text{I-T}}(t)\right]_{\|\mathbb{U}_N\|\times 1}\right]. \tag{16}$$

(iv) *Pseudo inputs*: $R_{ij}^{\text{D}}(t)$ and $q_{ij}^{p^{W-}}(t)$, $\forall i \in \mathbb{R}$ and $j \in \mathbb{U}_i$, are the pseudo inputs in the developed model. $R_{ij}^{\text{D}}(t)$ is the rate of cancellation of dispatched trips in Region i with pickup location in Region j (see Eqs. (3) and (4)). $q_{ij}^{p^{W-}}(t)$ is the cancellation rate of waiting passengers in Region i with destinations in Region j at time t because of their dissatisfaction with the ride-sourcing system (see Eqs. (8) and (9)). The values of these memory-less variables are affected by the vehicle–passenger matching method at each time instant. These inputs cannot be directly manipulated by dispatching and transfer subsystems and are not independent of the state variable. The pseudo inputs are:

$$\begin{aligned}
&\boldsymbol{U}^{\text{ps}}(t) = [\boldsymbol{Q}^{p^{W-}}(t), \boldsymbol{R}^{\text{D}}(t)] \qquad \boldsymbol{U}^{\text{ps}}(t) \subset \mathcal{R}^{2(N+\sum_{i=1}^{N}\|\mathbb{U}_i\|)},\\
&\boldsymbol{Q}^{p^{W-}}(t) = \left[\left[q_{1k_1}^{p^{W-}}(t)\right]_{\left(1+\|\mathbb{U}_1\|\right)\times 1}, \dots, \left[q_{ik_i}^{p^{W-}}(t)\right]_{\left(1+\|\mathbb{U}_i\|\right)\times 1}, \dots, \left[q_{Nk_N}^{p^{W-}}(t)\right]_{\left(1+\|\mathbb{U}_N\|\right)\times 1}\right],\\
&\boldsymbol{R}^{\text{D}}(t) = \left[\left[R_{1k_1}^{\text{D}}(t)\right]_{\left(1+\|\mathbb{U}_1\|\right)\times 1}, \dots, \left[R_{ik_i}^{\text{D}}(t)\right]_{\left(1+\|\mathbb{U}_i\|\right)\times 1}, \dots, \left[R_{Nk_N}^{\text{D}}(t)\right]_{\left(1+\|\mathbb{U}_N\|\right)\times 1}\right].
\end{aligned} \tag{17}$$

After defining the state variables and the inputs of the system, we can formulate the nonlinear state–space form of the model as

$$\frac{\mathrm{d}\boldsymbol{X}(t)}{\mathrm{d}t} = f\left(\boldsymbol{X}(t), \boldsymbol{U}^{\text{ex}}(t), \boldsymbol{U}^{\text{en}}(t), \boldsymbol{U}^{\text{co}}(t), \boldsymbol{U}^{\text{ps}}(t)\right), \tag{18}$$

where $f(.) : \mathcal{R}^{6N+5\sum_{i=1}^{N}\|\mathbb{U}_i\|} \times \mathcal{R}^{3N+\sum_{i=1}^{N}\|\mathbb{U}_i\|} \times \mathcal{R}^{3(N+\sum_{i=1}^{N}\|\mathbb{U}_i\|)} \times \mathcal{R}^{\sum_{i=1}^{N}\|\mathbb{U}_i\|} \times \mathcal{R}^{2(N+\sum_{i=1}^{N}\|\mathbb{U}_i\|)} \rightarrow \mathcal{R}^{6N+5\sum_{i=1}^{N}\|\mathbb{U}_i\|}$ is a continuous differentiable map (see Eqs. (1) to (11)). The transfer subsystem manipulates $\boldsymbol{U}^{\text{co}}(t)$ to regulate the state variables to satisfy a defined objective function. $\boldsymbol{U}^{\text{co}}(t) = 0$ reflects a ride-sourcing system without transfer subsystems. The following section introduces the NMPC as the repositioning controller.

3. Nonlinear model predictive controller design

In this section, we introduce the NMPC as the repositioning controller of the proposed ride-sourcing system. The interconnection between the dispatching subsystem, Plant, and the NMPC is illustrated in Fig. 1. The model predictive controller optimizes the future behavior of the system. To this end, the controller is required to predict the system's state variables. The prediction is determined based on the validated model (see Part I) paper and its corresponding nonlinear state–space representation (see Eq. (18)). The nonlinear state–space model for predicting the state variables needs the pseudo inputs, estimated values of the exogenous inputs, $\hat{\boldsymbol{U}}^{\text{ex}}(t)$, and estimated values of endogenous inputs $\hat{\boldsymbol{U}}^{\text{en}}(t)$. Estimated values of exogenous inputs are determined by applying exponential moving average on previous values of the exogenous inputs to smooth the noisy values. To increase the controllability of the model, we determine the estimated values of endogenous inputs k steps ahead, $\hat{\boldsymbol{U}}^{\text{en}}(t+k)$, as a function of the predicted state variables, $\boldsymbol{X}(t+k); k>0$ (see Section 3.2).

The predicted values of the state variables and constraints are fed to the optimization problem to minimize the defined cost function (see Eq. (19)). The NMPC is not based on the specifications of the dispatching subsystem; hence, the designed NMPC can be integrated with any dispatching subsystems. The NMPC produces the desired rates of *inter-regional* vehicle transfers. Then the *Link-Level Allocation* uses this output to recommend hot spot *streets* to reposition idle vehicles.

In the following, first, we define the cost function and constraints of the controller. In the second part, we propose estimations of the endogenous inputs during the prediction horizon to improve the controllability and proactiveness of the controller.

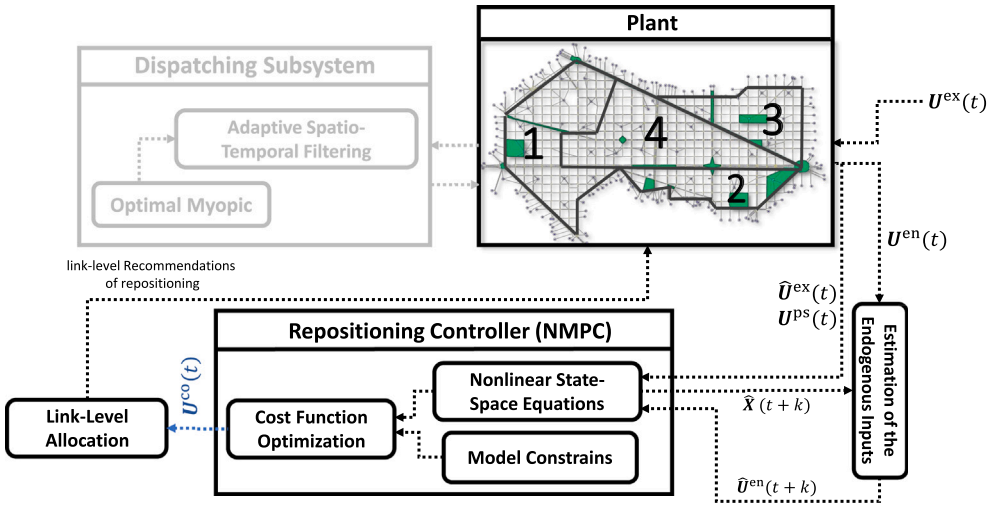

Fig. 1. Interaction between the Repositioning Controller and the Plant. (Note that the focus of this paper is not the dispatching subsystem; hence it is illustrated with lighter shades.) The exogenous demand of the trip requests and incoming vehicles are generated in the traffic network defined by $\boldsymbol{U}^{\mathrm{ex}}(t)$. The estimation of the predicted vehicle–passenger matchings, $\hat{\boldsymbol{U}}^{\mathrm{en}}(t+k)$, the cancellation rate of the dispatched vehicles and passengers' trip requests, $\boldsymbol{U}^{\mathrm{ps}}(t)$, and estimated values of the exogenous inputs, $\hat{\boldsymbol{U}}^{\mathrm{ex}}(t)$, are utilized in nonlinear state–space equations to predict the state variables, $\boldsymbol{X}(t+k)$. The set of controller inputs, $\boldsymbol{U}^{\mathrm{co}}(t)$, are determined by solving the constrained optimization problem.

3.1. Cost function and constraints

The repositioning controller (i.e., the transfer subsystem) aims to reposition idle vehicles to the regions with an excess number of passengers to increase the possibility of successful matchings in the future. The NMPC solves the finite-horizon optimal control problem at every transferring time instance. The NMPC solves Eq. (19) to control the rate of transferring vehicles, $\boldsymbol{U}^{\mathrm{co}}(t)$, to minimize the total *predicted* unassigned time of the vehicles (i.e., the difference between drop-off time and the subsequent matching time) and total *predicted* unassigned time of the passengers (i.e., the time that passengers remain unmatched in the network).

$$\begin{aligned}&\min_{\boldsymbol{U}^{\mathrm{co}}(t),\ldots,\boldsymbol{U}^{\mathrm{co}}(t+(n_{\mathrm{c}}-1)\times\Delta t_{\mathrm{pr}})} J\left(\boldsymbol{X}(t),\boldsymbol{U}^{\mathrm{ex}}(t),\boldsymbol{U}^{\mathrm{en}}(t),\boldsymbol{U}^{\mathrm{co}}(t)\right)\\ &=\min_{\boldsymbol{U}^{\mathrm{co}}(t_{\mathrm{tr}}),\ldots,\boldsymbol{U}^{\mathrm{co}}(t_{\mathrm{tr}}+(n_{\mathrm{c}}-1)\times\Delta t_{\mathrm{pr}})}\int_{t_{\mathrm{tr}}}^{t_{\mathrm{tr}}+n_{\mathrm{p}}\times\Delta t_{\mathrm{pr}}}\left[\boldsymbol{C}^{\mathrm{I}}(t),\boldsymbol{C}^{\mathrm{T}}(t),\boldsymbol{P}^{\mathrm{W}}(t)\right]\boldsymbol{Q}\left[\boldsymbol{C}^{\mathrm{I}}(t),\boldsymbol{C}^{\mathrm{T}}(t),\boldsymbol{P}^{\mathrm{W}}(t)\right]^{\top}\mathrm{d}t,\end{aligned}\tag{19}$$

where $\boldsymbol{Q}=\mathrm{diag}(\boldsymbol{Q}^{\mathrm{I}},\boldsymbol{Q}^{\mathrm{T}},\boldsymbol{Q}^{\mathrm{W}})$. $\boldsymbol{Q}^{\mathrm{I}}\subset\mathcal{R}^{N}$, $\boldsymbol{Q}^{\mathrm{T}}$ and $\boldsymbol{Q}^{\mathrm{W}}\subset\mathcal{R}^{N+\sum_{i=1}^{N}\|\mathbb{U}_i\|}$ are symmetric positive semidefinite matrices for weighting contributions of idle vehicles, transfer vehicles, and waiting passengers in the cost function, respectively. These matrices can be used to regulate the significance of vehicles (drivers) and passengers for the ride-sourcing company. $\int \boldsymbol{C}^{\mathrm{I}}(t)\boldsymbol{Q}^{\mathrm{I}}\boldsymbol{C}^{\mathrm{I}^{\top}}(t)+\boldsymbol{C}^{\mathrm{T}}(t)\boldsymbol{Q}^{\mathrm{T}}\boldsymbol{C}^{\mathrm{T}^{\top}}(t)\mathrm{d}t$ formulates the weighted square of the total predicted waiting time of the vehicles. The total predicted waiting time of the passengers is denoted by $\int \boldsymbol{P}^{\mathrm{W}}(t)\boldsymbol{Q}^{\mathrm{W}}\boldsymbol{P}^{\mathrm{W}^{\top}}(t)\mathrm{d}t$. t_{tr} is the transfer time instance and $n_{\mathrm{p}}\times\Delta t_{\mathrm{pr}}$ is the prediction duration. Δt_{pr} denotes the prediction sample and n_{p} is the prediction horizon. We can utilize the control horizon of n_{c} time steps to optimize only the first n_{c} steps of the transfer actions ($n_{\mathrm{c}}\leq n_{\mathrm{p}}$). This reduces the computational efforts for solving the optimization problem.

At each transfer time instance, the NMPC uses feedback from the ride-sourcing system to obtain the state variables, $\boldsymbol{X}(t_{\mathrm{tr}})$, exogenous inputs, $\boldsymbol{U}^{\mathrm{ex}}(t_{\mathrm{tr}})$, and endogenous inputs, $\boldsymbol{U}^{\mathrm{en}}(t_{\mathrm{tr}})$. The NMPC uses these values as the initial value of the prediction and utilizes the developed model (see Eq. (18)) to make predictions of the system's state up to time $t_{\mathrm{tr}}+n_{\mathrm{p}}\times\Delta t_{\mathrm{pr}}$. It solves the optimization problem to find the sequence of optimum transfer actions, $\left[\boldsymbol{U}^{\mathrm{co}^*}(t_{\mathrm{tr}}),\boldsymbol{U}^{\mathrm{co}^*}(t_{\mathrm{tr}}+\Delta t_{\mathrm{pr}}),\ldots,\boldsymbol{U}^{\mathrm{co}^*}(t_{\mathrm{tr}}+(n_{\mathrm{c}}-1)\times\Delta t_{\mathrm{pr}})\right]$, that minimizes the total predicted unassigned time. The solution of the optimization problem must satisfy Constraints (20a)–(20c). Afterward, only the first step of the obtained optimum transfer actions is applied for transferring idle vehicles, $\boldsymbol{U}^{\mathrm{co}^*}(t_{\mathrm{tr}})$.

$$\boldsymbol{X}(t)\geq 0 \qquad t\in[t_{\mathrm{tr}},t_{\mathrm{tr}}+n_{\mathrm{p}}\times\Delta t_{\mathrm{pr}}],\tag{20a}$$

$$\boldsymbol{U}^{\mathrm{co}}(t)\geq 0 \qquad t\in[t_{\mathrm{tr}},t_{\mathrm{tr}}+n_{\mathrm{p}}\times\Delta t_{\mathrm{pr}}],\tag{20b}$$

$$c_i^{\mathrm{I}}(t)+\sum_{j\in\{\mathbb{U}_i,i\}}\left(c_{ij}^{\mathrm{T}}(t)+c_{ij}^{\mathrm{D}}(t)+c_{ij}^{\mathrm{O}}(t)\right)\leq n_i^{\mathrm{jam}}-n_i(t_{\mathrm{tr}}) \quad t\in[t_{\mathrm{tr}},t_{\mathrm{tr}}+n_{\mathrm{p}}\times\Delta t_{\mathrm{pr}}],\ \forall i\in\mathbb{R},\tag{20c}$$

where $n_i(t_{\mathrm{tr}})$ is the total number of non-ride-sourcing vehicles in Region i at time t_{tr}. Since the model does not track the evolution of the number of non-ride-sourcing vehicles, we assume that this number remains fixed during the prediction horizon. At each transferring time, this number is updated by feedback from the system. Constraints (20a) and (20b) ensure all the state variables and optimum transferring rates are non-negative. Constraint (20c) sets an upper limit on the total number of vehicles in each

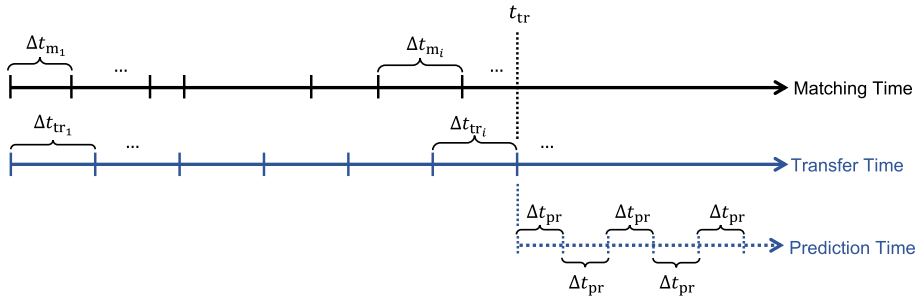

Fig. 2. The matching, transfer, and prediction sample times.

region. An upper bound for each state variable can be set easily to enforce the optimum transferring rates aligned with the ride-sourcing company's policies. For more details about MPC and its use in ride-sourcing systems and traffic control and pricing, see for example Ramezani and Nourinejad (2018), Yildirimoglu et al. (2018), Sirmatel and Geroliminis (2021), Haddad and Mirkin (2021), Li and Ramezani (2022).

The optimization problem (19) is solved by the interior point method that combines line search and trust region steps. The primary step in this method is line search using direct linear algebra. If the problem is not convex or there is a singularity in Jacobian and Hessian, then the primary step will be replaced by trust region step. This replacement of trust region step guarantees optimization progress when the line search step fails. In this method, Karush–Kuhn–Tucker (KKT) approach is used to consider the equality and inequality constraints (Waltz et al., 2006). This solver is available in KNITRO (Byrd et al., 2006) and MATLAB and the computational efficiency of this solver is well-studied in Wächter and Biegler (2006).

3.2. Estimation of the endogenous inputs

We consider three sampling times in the system: matching, transfer, and prediction clocks. As depicted in Fig. 2, the matching frequency, Δt_{m_i}, is time-varying. The matching frequency in this paper is determined from the proposed adaptive spatio-temporal matching method in Part I paper. In this study, we assume the frequency of transferring is time-invariant. To set the transferring frequency, it is crucial to take into account the average number of rejections determined by the adaptive spatio-temporal filtering. The higher the number of rejections, the higher the number of idle vehicles available for repositioning. The prediction frequency is introduced to discretize the continuous model (Eq. (18)) for predicting of the state variables. At each transfer time, t_{tr}, we assume prediction sampling time, Δt_{pr}, is time-invariant.

Let us assume the transfer subsystem is executed at time t_{tr}. The endogenous inputs (e.g., the rate of the idle/transferred vehicles to be matched to the waiting passengers) and pseudo inputs are known at any time before $t \le t_{tr}$. The pseudo inputs are not dominant inputs significantly impacting the operating point of the system and intrinsically are stochastic processes because they reflect human preferences. Hence, we consider them as disturbances in designing the NMPC. The dominant endogenous inputs are *not known* during the prediction time, $t \in (t_{tr}, t_{tr}+n_p \times \Delta t_{pr}]$. In addition, the evolution of the model's state variables is a function of the endogenous inputs, and their availability is necessary for predicting the state variables. Our experiments show that the state–space model formulation becomes uncontrollable if these inputs are assumed to be fixed during the prediction interval. The reason is that the effect of manipulating control inputs, $\boldsymbol{U}^{co}(t)$, cannot be reflected in the rate of the vehicle–passenger matching during the prediction interval. To address this issue, let us denote

$$m^{\text{myopic}}(t) = \min\Big(\sum_{i\in\mathbb{R}} c_i^{\text{I}}(t) + \sum_{i\in\mathbb{R}}\sum_{j\in\{\mathbb{U}_i,i\}} c_{ij}^{\text{T}}(t), \sum_{i\in\mathbb{R}}\sum_{j\in\{\mathbb{U}_i,i\}} p_{ij}^{\text{W}}(t)\Big) \quad t \in [t_{tr}, t_{tr}+n_p\times\Delta t_{pr}], \tag{21}$$

$$r = \frac{m^{\text{plant}}(t_{tr})}{m^{\text{myopic}}(t_{tr})}, \tag{22}$$

where $m^{\text{plant}}(t_{tr})$ represents the number of the vehicle–passenger matchings at time t_{tr} (with considering rejection), and $m^{\text{myopic}}(t)$ denotes the number of the matchings without considering rejection. The rejection ratio $0 \le r \le 1$ is assumed to be constant during the prediction interval. At each transfer time instance, the NMPC uses the feedback from the system to update $m^{\text{plant}}(t_{tr})$ and $m^{\text{myopic}}(t_{tr})$ to update the rejection ratio.

The endogenous inputs during the prediction interval can be estimated as Eqs. (23)–(25).

$$\widehat{W}_{ij}^{\text{I-D}}(t) = \frac{\sum_{i\in\{\mathbb{U}_j,i\}} p_{ji}^{\text{W}}(t)}{\sum_{i\in\mathbb{R}}\sum_{j\in\{\mathbb{U}_i,i\}} p_{ij}^{\text{W}}(t)} \frac{c_i^{\text{I}}(t)}{\sum_{i\in\mathbb{R}} c_i^{\text{I}}(t) + \sum_{i\in\mathbb{R}}\sum_{j\in\{\mathbb{U}_i,i\}} c_{ij}^{\text{T}}(t)} \times r \times \frac{m^{\text{myopic}}(t)}{\Delta t_{pr}} \quad t \in [t_{tr}, t_{tr}+n_p\times\Delta t_{pr}], \tag{23}$$

$$\widehat{W}_{ij}^{\text{T-D}}(t) = \frac{\sum_{i\in\{\mathbb{U}_j,i\}} p_{ji}^{\text{W}}(t)}{\sum_{i\in\mathbb{R}}\sum_{j\in\{\mathbb{U}_i,i\}} p_{ij}^{\text{W}}(t)} \frac{\sum_{j\in\{\mathbb{U}_i,i\}} c_{ij}^{\text{T}}(t)}{\sum_{i\in\mathbb{R}} c_i^{\text{I}}(t) + \sum_{i\in\mathbb{R}}\sum_{j\in\{\mathbb{U}_i,i\}} c_{ij}^{\text{T}}(t)} \times r \times \frac{m^{\text{myopic}}(t)}{\Delta t_{pr}} \quad t \in [t_{tr}, t_{tr}+n_p\times\Delta t_{pr}], \tag{24}$$

$$\widehat{W}_{ij}^{\text{W-A}}(t) = \frac{p_{ij}^{\text{W}}(t)}{\sum_{i\in\mathbb{R}}\sum_{j\in\{\mathbb{U}_i,i\}} p_{ij}^{\text{W}}(t)} \times r \times \frac{m^{\text{myopic}}(t)}{\Delta t_{\text{pr}}} \quad t \in [t_{\text{tr}}, t_{\text{tr}}+n_{\text{p}}\times\Delta t_{\text{pr}}]. \tag{25}$$

$\widehat{W}_{ij}^{\text{I-D}}(t)$ and $\widehat{W}_{ij}^{\text{T-D}}(t)$ respectively denote the estimated rate of idle and transferred vehicles with current locations in Region i that become dispatched in Region j (the origin of the passenger is in Region j) at time t. $\widehat{W}_{ij}^{\text{W-A}}(t)$ is the estimated rate of waiting passengers with pick up locations in Region i and drop off locations in Region j at time t who become assigned. The first terms in RHS of Eqs. (23) and (24) are the total number of waiting passengers in Region j normalized with respect to the total number of waiting passengers in the network. This ratio reflects the portion of the dispatched vehicles to Region j. The second terms in RHS of Eqs. (23) and (24) reflect the portion of the idle and the transferred vehicles, respectively, that the dispatched vehicles are selected from. The last two terms in RHS of Eqs. (23) to (25) estimate the rate of matchings with rejections.

4. Microsimulation experiments

In this section, we introduce the traffic microsimulation case study and illustrate the results under 3 settings. In the first setting, there is no transfer subsystem. In the second setting, we use a reactive controller as in Section 4.2. The reactive controller is developed based on transferring the vehicles to the regions with a higher instantaneous number of waiting passengers. The third setting uses the NMPC as the transfer subsystem that considers the effect of the transferring on the future evolution of the state variables. We utilize the adaptive spatio-temporal matching introduced in Part I paper as the dispatching subsystem in all the settings. Hence, the discarded vehicles by the matching method and new idle vehicles are considered as potential idle vehicles for transferring to neighbor regions. In these experiments, the only difference between all the settings is the transfer subsystem.

In the following, we compare the evolution of the idle, transferred, dispatched, and occupied vehicles and waiting and assigned passengers for each transfer subsystem setting. Moreover, we compare the performance of each setting with respect to passengers' and vehicles' unassigned time, passengers' and vehicles' waiting time, the number of trip cancellations, and the number of impatient drivers who leave the system because of not being matched to passengers for an excessive time.

4.1. Case study

We scrutinize the efficiency of the proposed transferring controller with a traffic microsimulation. To this end, we develop a ride-sourcing testbed in Aimsun in which ride-sourcing vehicles and travel demands fully interact with other modes of traffic (private vehicles and buses). This microsimulation setup includes point-to-point routing of ride-sourcing vehicles, assigning vacant vehicles (i.e., transfer and idle vehicles) to waiting passengers, managing the generation of incoming ride-sourcing vehicles, and simulating passenger travel requests. Routing of the vehicles is determined by finding the shortest travel time path between the designated origin and destination. In this study, we utilize the adaptive spatio-temporal matching method described in Part I paper for assigning vacant vehicles to waiting passengers with 60 [s] and 5 [s] set as the upper and lower bounds of the matching interval. New idle ride-sourcing vehicles and waiting passengers join the network as shown in Fig. 3. A stochastic time threshold is considered for all the idle ride-sourcing vehicles and waiting passengers to model their impatient characteristics. If a driver remains vacant or a waiting passenger is not picked up before their patience time, they leave the ride-sourcing system or cancel their trip request because of unsatisfactory quality of service. Each driver's and passenger's stochastic and unique patience time thresholds are randomly selected from normal distributions with predefined means and variances.

To investigate the effectiveness of the NMPC as the transfer subsystem, we apply the proposed controller on the calibrated traffic microsimulation model of part of Barcelona that is partitioned into four regions as in Kouvelas et al. (2017). To this end, we set the transfer cycle equal to 60 [s] to assure there are sufficient idle vehicle candidates for transferring. An imbalanced supply–demand scenario is created by setting the exogenous rate of the travel requests (i.e., the arrival of waiting passengers) and the exogenous rate of arrival of new ride-sourcing vehicles, as in Fig. 3. In this figure, during $[1800, 4500]$ and $[6300, 10800]$, most travel requests have origins and destinations in Region 3 and Region 2, respectively. Since Region 2 and Region 3 are far from each other (see Fig. 1), the distances between the majority of idle vehicles and waiting passengers are greater than the maximum matching distance obtained from the adaptive spatio-temporal matching method. In each transfer time instance, the exogenous inputs are estimated during the prediction horizon with exponential smoothing. The weight is set to 0.7, and the initial condition of the smoothed value is set to the initial value of the exogenous inputs at the beginning of each transfer time instance.

4.2. Reactive transferring

In this part, we introduce a model-free reactive controller as a benchmark method to scrutinize the proactiveness of the NMPC. The reactive controller uses the instantaneous number of idle vehicles and waiting passengers at each transferring time to determine the desired number of idle vehicles in each region. Then, it calculates the repositioning rates of idle vehicles between regions to achieve the desired number of idle vehicles in each region. The desired number of idle vehicles in Region i at time t, $c^{*\text{I}}_i(t)$, is obtained by solving the following constrained optimization:

$$\begin{aligned} &\min_{c^{*\text{I}}_1(t),\ldots,c^{*\text{I}}_N(t)} \left(\sum_{i\in\mathbb{R}}\left(c^{*\text{I}}_i(t) - \sum_{j\in\{\mathbb{U}_i,i\}} p_{ij}^{\text{W}}(t)\right)\right)^2 \\ &\text{s.t.} \quad \sum_{i\in\mathbb{R}} c^{*\text{I}}_i(t) = \sum_{i\in\mathbb{R}} c^{\text{I}}_i(t). \end{aligned} \tag{26}$$

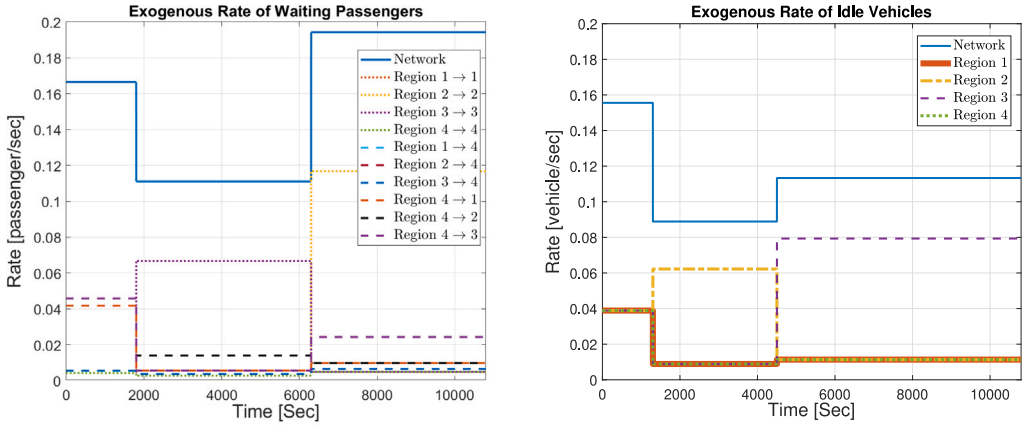

Fig. 3. Arrival rate of new (a) waiting passengers and (b) idle vehicles who join the ride-sourcing system.

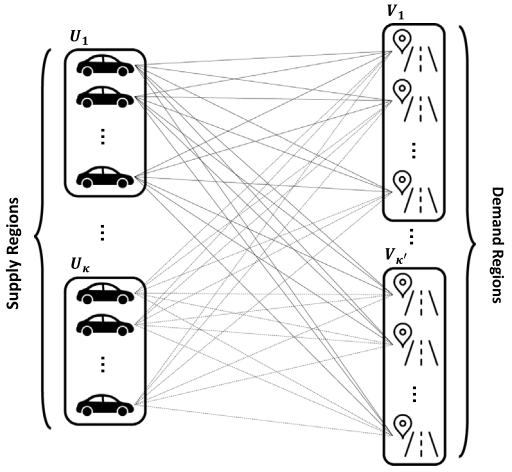

Fig. 4. The bipartite graph for transferring idle vehicles to candidate locations that is obtained from the reactive controller.

Eq. (26) determines the number of desired idle vehicles such that the difference between idle vehicles and waiting passengers becomes minimum in all regions. This avoids long-distance matchings (i.e., reducing the rejection rate of vehicle–passenger matchings). The constraint is that the total number of desired idle vehicles must be equal to the total number of idle vehicles in the ride-sourcing system at time t.

To reach the desired spatial distribution as in Eq. (26), a subset of idle vehicles in each region are advised to transfer to other regions. To this end, we need to determine the transferring origin (i.e., choosing a designated idle vehicle for transferring) and the destination for each designated idle vehicle. Transferring origins and destinations are obtained by solving heuristically an integer optimization problem that is equivalent to finding a subset of a maximum matching of a bipartite graph. In this problem, each side of the bipartite graph is partitioned into a set of disjoint subsets (i.e., supply and demand) (see Fig. 4). A subset is defined as a *supply* region if there is an excess number of idle vehicles, $c^{*\mathrm{I}}_i(t) - c^{\mathrm{I}}_i(t) < 0$, and is defined as a *demand* region if there is a shortage of idle vehicles, $c^{*\mathrm{I}}_i(t) - c^{\mathrm{I}}_i(t) > 0$. If the current number of idle vehicles in each region equals the desired number of idle vehicles, the reactive controller does not send in or send out any idle vehicles.

The bipartite graph as depicted in Fig. 4, $G(U, V, E)$, has two sets of vertices (i.e., supply, U, and demand, V) and one set of edges E. Each edge $e=(u,v)\in E, u\in U, v\in V$ has a weight, $w(e)$. The set of supply vertices, U, is partitioned into κ disjoint subsets where κ is the number of supply regions, $U_1, \ldots, U_\kappa$. The set of demand vertices, V, is partitioned into κ' disjoint subsets that κ' is the number of supply regions, $V_1, \ldots, V_{\kappa'}$.

The cardinality of each subset is

$$\|U_i\| = c^{\mathrm{I}}_i(t) \quad i \in \{1, \ldots, \kappa\};\ \|V_i\| = c^{*\mathrm{I}}_i(t) - c^{\mathrm{I}}_i(t) \quad i \in \{1, \ldots, \kappa'\} \quad . \tag{27}$$

Each supply region has $c_i^{\mathrm{I}}(t) - c^{*\mathrm{I}}_i(t)$ excess idle vehicles that must be transferred to locations in demand regions. Each demand region needs $c^{*\mathrm{I}}_i(t) - c_i^{\mathrm{I}}(t)$ idle vehicles to be transferred from supply regions. Nodes in Fig. 4 in the demand regions are candidate locations (i.e., destinations of transferring). The candidate locations are chosen randomly around the geometric center of available waiting passengers of the demand region. Nodes in Fig. 4 in supply regions are the current location of idle vehicles (i.e., origins of transferring). The weights, $w(e, v)$, of the graph are negative of the shortest travel time between the idle vehicles in supply regions and the candidate locations in the demand regions determined by the Dijkstra algorithm. The maximum matching in each supply subset, U_i, is $c_i^{\mathrm{I}}(t) - c^{*\mathrm{I}}_i(t)$. By solving subsets of maximum matching of G (Barketau et al., 2015), we determine pairs of origins and destinations for transferring idle vehicles at each transferring time.

4.3. Evolution of the ride-sourcing system state

In this part, the evolution of the number of different groups of vehicles (idle, dispatched, occupied, and transferred) and passengers (waiting and assigned) are depicted for the center region (Region 4) and the surrounding regions (Regions 1, 2, and 3). The center region has borders with all the surrounding regions, but the surrounding regions have no borders with each other, see Fig. 1. We investigate the effect of transfer subsystem using no transferring, the reactive controller, and the NMPC. The ride-sourcing system under all settings utilizes the adaptive spatio-temporal matching method. The frequency of the transfer subsystem is fixed at 60 [s]. The results of the NMPC is reported by setting $n_{\mathrm{c}} = 2$, $n_{\mathrm{p}} = 30$, and $\Delta t_{\mathrm{pr}} = 15$ [s]. Choosing a proper value for the prediction and control horizons depends on the dynamic of the system. There is a trade-off in choosing the prediction horizon: selecting a very low value for the prediction horizon results in a reactive controller; however, setting a very large value for the prediction horizon results in the overlook of and the inability to regulate the transient behavior of the system. The control horizon manipulates the complexity of the optimization problem. We set the control horizon equal to 2 to reduce the complexity.

Fig. 5 shows the evolution of the number of waiting passengers and idle vehicles using no transferring, the reactive controller, and the NMPC. At the start of the test, there is an excess number of idle vehicles and waiting passengers simultaneously, which shows the high number of long-distance rejections in the center region (i.e., Region 4). The high number of long-distance rejections stems from the fact that most travel requests are generated in the central region, but the idle vehicles are distributed uniformly in the center and surrounding regions (see Fig. 3). Based on Figs. 5.a, 5.b, and 5.c, the numbers of waiting passengers at the beginning of the tests are the same despite the transferring settings. However, the numbers of idle vehicles by using the reactive controller or the NMPC are smaller than the no transferring setting (see Figs. 5.d, 5.e, and 5.f) because some of the idle vehicles become transferred.

During time $[0, 1500]$ (samples 0 to 100), the number of waiting passengers decreases in the center region (i.e., Region 4) in all settings because of two reasons (i) more ride-sourcing vehicles join the system and (ii) Region 4 is at the center of the network and has a border with other regions such that vehicles in the surrounding regions can be matched to waiting passengers in the central region with a high possibility. The decreasing rate of the number of waiting passengers in the center region by using the proposed NMPC is higher than the reactive controller and the no transferring setting (see Figs. 5.a, 5.b, and 5.b) that is the result of well positioning of the vacant vehicles by the transfer subsystem.

Fig. 5 shows that there is an excess number of waiting passengers in Region 2 and idle vehicles in Region 3 after time 6150 [s] (sample 410) because (i) there is an abrupt change in passengers' trip requests in Region 2 with a destination in Region 2 (see Fig. 3.a) and (ii) the rate of exogenous idle vehicles increases drastically in Region 3 after time 4500 [s] (sample 300) as depicted in Fig. 3.b. We see that in Figs. 5.a and 5.d after time 6150 [s] (sample 410), the number of waiting passengers and the number of idle vehicles are higher than the case when the reactive controller or the NMPC is used. This is because Region 3 and Region 2 are far from each other and the adaptive spatio-temporal matching method discards the majority of vehicle–passenger matchings between waiting passengers in Region 2 and idle vehicles in Region 3. Figs. 5.b, 5.c, 5.e, and 5.f illustrate that the reactive controller and the NMPC shrink the imbalance between waiting passengers and idle vehicles by reducing the number of waiting passengers in Region 2 and idle vehicles in Region 3. Fig. 6 shows the number of transferring vehicles in each region at time t. This figure depicts that the excess idle vehicles in Region 3 and Region 4 have been transferred to increase the probability of being matched to the waiting passengers in Region 2.

Fig. 7 shows the non-zero transferring rates of idle vehicles by the NMPC. The total number of repositioning trips with the reactive controller and the NMPC are 422 and 526, respectively. The NMPC transfers the vehicles from the surrounding regions (i.e., Regions 1, 2, and 3) to the center region (i.e., Region 4). In this figure, during $[0, 3750]$ (samples 0 to 250), the rate of vehicles that are transferred from Region 2 to the central region increases. This is because in period $[0, 1800]$ (samples 0 to 120) the exogenous rate of waiting passengers from Region 4 to Region 2 is relatively high (see Fig. 3.a), which results in accumulation of idle vehicles in Region 2 (ride-sourcing vehicles pickup passengers in Region 4 and drop them off in Region 2 and become idle in Region 2). Furthermore, at time 1200 [s] (sample 80) the rate of new (exogenous) idle vehicles in Region 2 increases significantly (see Fig. 3.b) and remains relatively high till 4500 [s] (sample 300). It amplifies the accumulation of idle vehicles in Region 2. After sample 460 in Fig. 6 (time 6900 [s]), the rate of vehicle transfer from Region 3 to Region 4 increases to compensate for (i) the excess of waiting passengers in Region 2 that is a result of the exogenous rate of waiting passengers from Region 2 to Region 2 (see Fig. 3.a) and (ii) excess of idle vehicles in Region 3 as a result of high exogenous rate of idle vehicles in Region 3 (see Fig. 3.b).

Fig. 8 illustrates the evolution of the number of dispatched vehicles, occupied vehicles, and assigned passengers in the system with no transferring method, the reactive controller, and the NMPC. During samples between 0 to 100, there are excess numbers of waiting passengers and idle vehicles in Region 4 (see Fig. 5). During this time, the total number of dispatched vehicles, Figs. 8.a, 8.b, and 8.c, (equivalent to the total number of assigned passengers, Figs. 8.g, 8.h, and 8.i) of reactive controller is relatively higher than

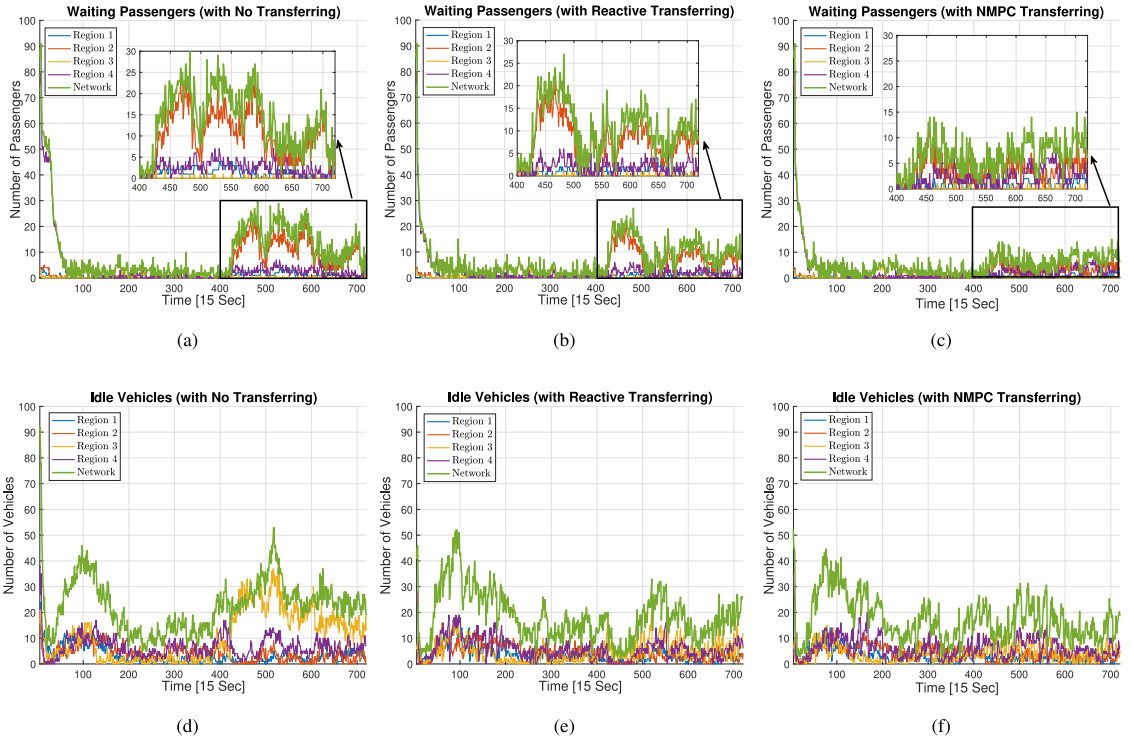

Fig. 5. Evolution of the number of waiting passengers and idle vehicles using different transferring methods. Waiting Passengers (a) without transferring, (b) with reactive transferring, and (c) with the NMPC transferring. Idle vehicles (d) without transferring, (e) with reactive transferring, and (f) with the NMPC transferring.

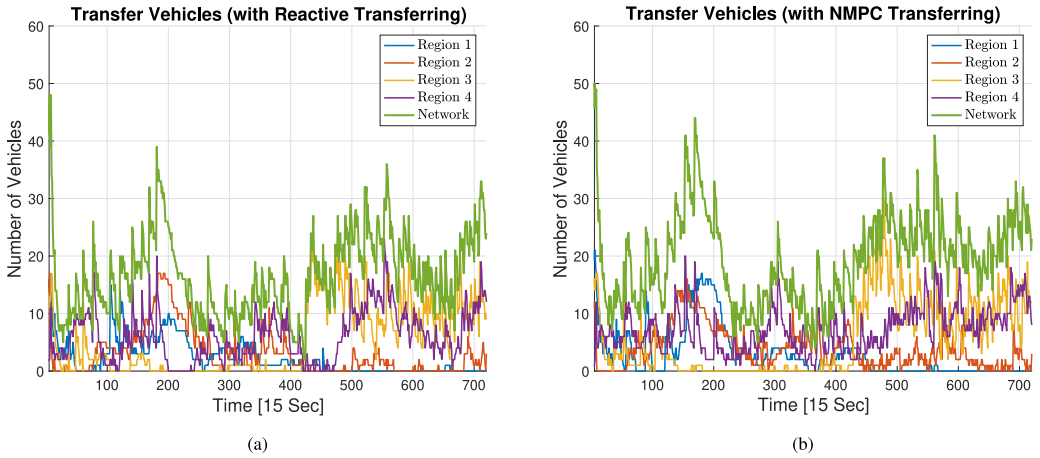

Fig. 6. Evolution of the number of transferring vehicles utilizing the (a) reactive controller and (b) NMPC. Each curve represents the number of transferring vehicles in each region. For example blue curve depicts the number of currently transferring vehicles from any region to any region that are currently in region 1.

with no transferring and the NMPC. However, during samples 60 to 200, the total number of occupied vehicles by using the NMPC is relatively higher than no transferring and the reactive controller. During this period, the mean values of occupied vehicles with no transferring, the reactive controller, and the NMPC are 54.3, 60.2, and 64.3, respectively. Moreover, after sample 400, when the transferring methods reduce the imbalance between idle vehicles in Region 3 and waiting passengers in Region 2, the mean values of the total number of occupied vehicles with no transferring, the reactive controller, and the NMPC are 70.4, 73.6, and 80.2, respectively. This is 13.9% and 8.9% improvements in the vehicle occupation rate by using the NMPC in comparison with no transferring and the reactive controller.

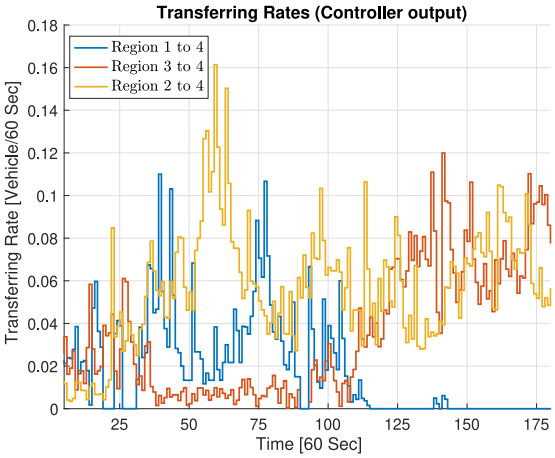

Fig. 7. The non-zero transferring rates implemented by the NMPC.

Table 1
The number of served passengers and operational fleet size for different settings of the transfer subsystem. Averages of five microsimulation replications is reported. Numbers in parenthesis show percentage of the variation with respect to no transferring method.

	Average number of served passengers	Average fleet size	Average Number of served passengers per vehicle
No transfer subsystem	1337	193	6.93
Reactive controller	1407 (5.2%)	178 (−7.7%)	7.90 (14.0%)
NMPC	1467 (9.7%)	157 (−18.6%)	9.34 (34.7%)

4.4. Served passengers and fleet size evaluation

In this part, we compare the three settings with respect to fleet size and the number of order cancellations. Each driver's stochastic patience time threshold is randomly generated from a normal distribution with mean value of 1200 [s] and variance of 600 [s^2]. Microsimulations with no controller, the reactive controller, and the NMPC result in 193 [veh], 178 [veh], and 157 [veh] unique ride-sourcing vehicles required to serve the same demand of trip requests (average of five microsimulation runs). It is equal to 7.7% and 18.6% reduction in required fleet size by using the reactive controller and the NMPC, respectively. Fig. 9.a represents the cumulative number of outgoing vehicles for one simulation replication (the vehicles that leave the system because of not being matched to passengers before drivers' patience time threshold). This figure illustrates that using the NMPC, a smaller number of ride-sourcing vehicles are needed to serve the passengers. Hence, a reduction in unnecessary search trips is expected that alleviates the overall network congestion level.

Furthermore, the total numbers of served passengers by averaging five simulation replications are 1337, 1407, and 1467 using no controller, the reactive controller, and the NMPC, respectively. This shows 5.2% and 9.7% increase in the number of served passengers by using the reactive controller and the NMPC, respectively. We adopt stochastic time-invariant values for passengers' patience time threshold. In these experiments, we choose a normal distribution with a mean value of 600 [s] and a variance of 135 [s^2] for the patience time of passengers. Fig. 9.b depicts the cumulative number of order cancellations in which the number of order cancellations by using the NMPC is less than using the reactive controller or with no transfer subsystem. If we focus on the reactive controller and with no transfer settings, we see that after sample 120 (7200 [s]), when the imbalance between idle vehicles and waiting passengers widens, using the reactive controller reduces the number of unserved passengers. Before sample 120, by using the reactive controller, the number of unserved passengers is higher than with no transfer subsystem. Nevertheless, the proactiveness of the NMPC reduces the number of unserved passengers throughout the simulation.

Table 1 presents the summary of comparison among no controller, the reactive controller, and the NMPC with respect to the number of served passengers and fleet size. The results are obtained by averaging five microsimulation replications. As illustrated in Table 1, the average numbers of served passengers by each vehicle are increased by 14.0% and 34.7% using the reactive controller and the NMPC, respectively. Note that the proposed adaptive spatio-temporal matching in Part I is used in the experiments summarized in Table 1. To isolate the effect of the proposed proactive transferring method from the adaptive spatio-temporal matching, Appendix discusses the results of experiments with the optimal myopic method with a fixed matching interval of 30 [s] and no discarding.

4.5. Delay comparison

Table 2 lists the performance of different transfer subsystems with respect to the passengers' unassigned time (the duration from placing a trip order to receiving a matching message with pickup information by the platform), vehicles' unassigned time (the idle

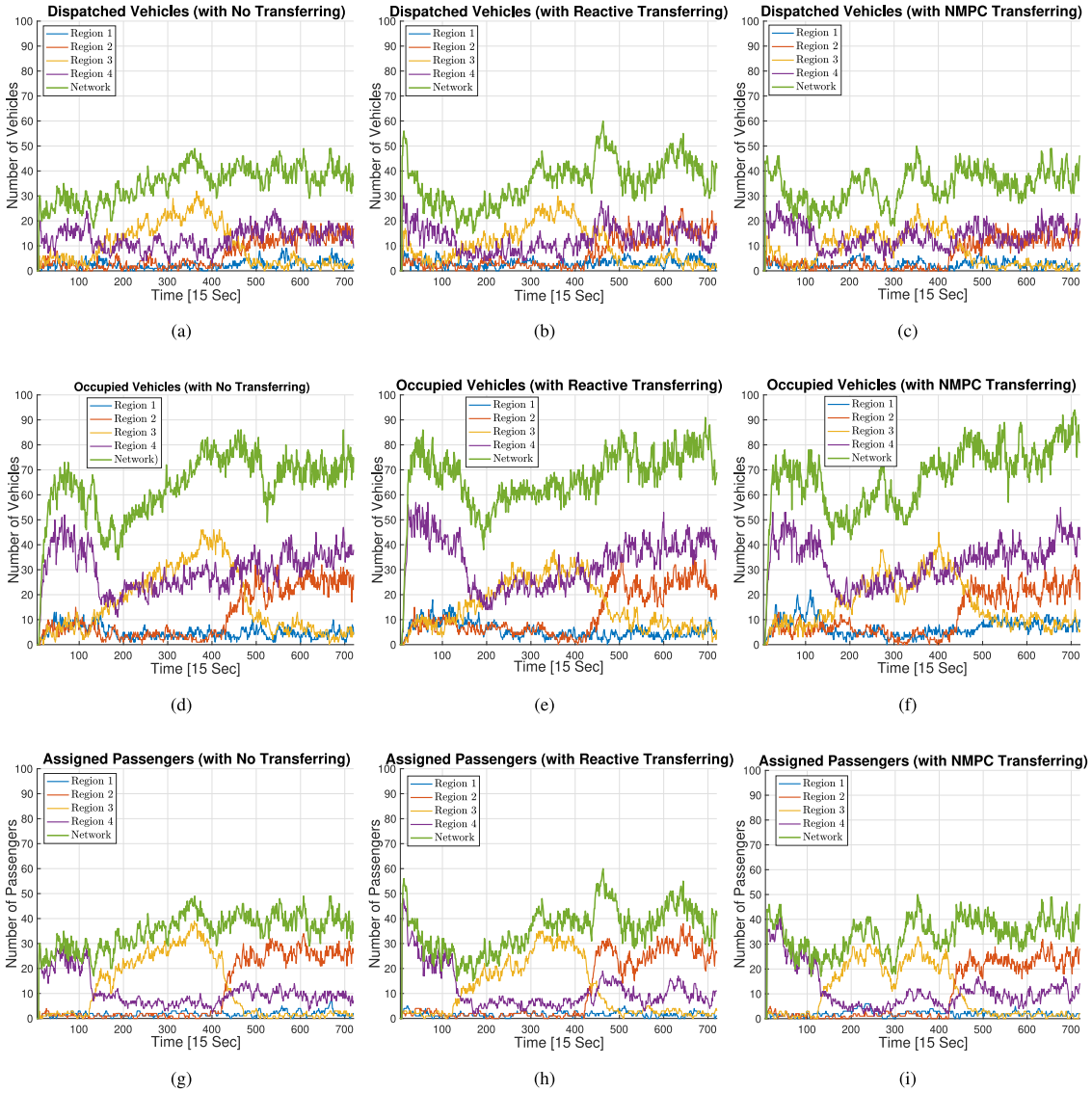

Fig. 8. Evolution of the number of dispatched vehicles, occupied vehicles, and assigned passengers using different transferring methods. Dispatched vehicles (a) without transferring, (b) with reactive transferring, and (c) with the NMPC transferring. Occupied vehicles (d) without transferring, (e) with reactive transferring, and (f) with the NMPC transferring. Assigned passengers (g) without transferring, (h) with reactive transferring, and (i) with the NMPC transferring.

duration), passengers' waiting time (the duration from placing a trip order to being picked up by a vehicle), and vehicles' waiting time (the duration a vehicle does not serve a passenger) for successful pickups.[1] Using the reactive controller and the NMPC, the vehicles' unassigned time increases. This is because transferring trips postpone immediate matching of the (excess) number of idle vehicles in favor of proactive balancing between new arriving waiting passengers and idle vehicles. Note that both the passengers' and vehicles' waiting times are reduced when using the NMPC. Because, instead of instantaneous matching, the transfer subsystem recommends vehicles to reposition to other regions for more efficient future matching (i.e., vehicles being closer to new arriving waiting passengers). The NMPC results in lower standard deviations of the reported measures, indicating higher equity among drivers and passengers.

[1] Note that the durations that vehicles transfer from one region to another are not included in the vehicles' unassigned time. Further, the difference between passenger waiting time and unassigned time (i.e., the pickup time) is much larger than that between vehicle waiting time and unassigned time. It is because transfer durations are included in the vehicles' waiting time.

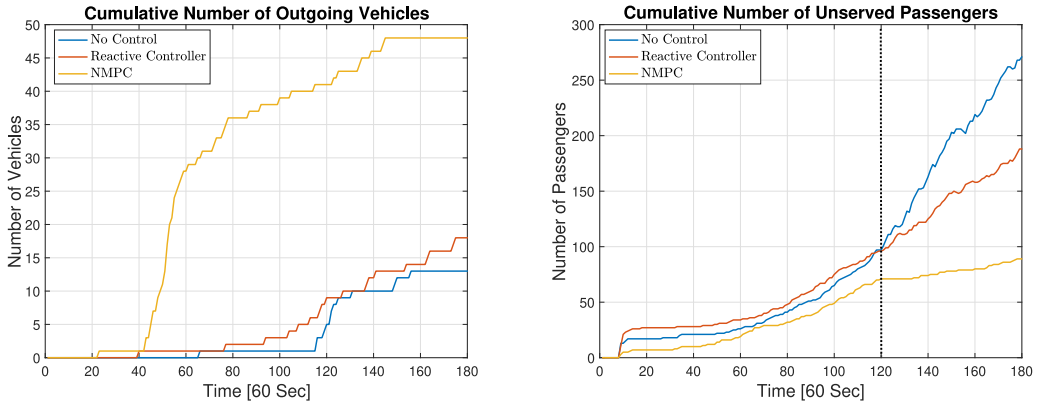

Fig. 9. Cumulative number of (a) outgoing vehicles and (b) order cancellations because of not being matched before passengers' patience time.

Table 2
Unassigned and waiting delays with no controller, the reactive controller, and the NMPC. Results are obtained by averaging five microsimulation replications. Numbers in parenthesis show the percentage of variation with respect to the no transferring method. Lower standard deviations indicate more equitable systems.

	Passengers' unassigned time [s]		Passengers' waiting time [s]		Vehicles' unassigned time [s]		Vehicles' waiting time [s]	
	Mean	SD	Mean	SD	Mean	SD	Mean	SD
No transfer subsystem	36	57	166	124	161	337	749	1200
Reactive controller	34 (−5.5%)	56	151.2 (−8.9%)	122	228 (40.7%)	501	736 (−1.9%)	1102
NMPC	28 (−20.4%)	47	146 (−12.4%)	116	174 (7.8%)	316	685 (−8.8%)	970

Ultimately, the NMPC leads to superior performance in terms of reducing the number of waiting passengers and increasing the rate of occupied vehicles in comparison with the reactive controller because the NMPC (i) considers the current location and *future destination* of different groups of vehicles and passengers and (ii) incorporates the short-term future effect of transferring.

4.6. Drivers incentives

In this part, we focus on the effect of the reactive controller and the NMPC on the traveled distance of transferred and dispatched vehicles. We show that drivers (contractors), by following the transferring commands of the ride-sourcing system, reduce their Guided Vacant Cruising Distance (GVCD), which is the sum of the transferred and dispatched distances of idle vehicles before each occupied trip. Figs. 10.b and 10.c depict the normalized histogram of the GVCD for the vehicles that have been transferred prior to being matched. Fig. 10.a illustrates the histogram of the GVCD with no transferring. In this figure, GVCD is reported for the vehicles that have received at least one transferring command in the NMPC setting. (This is to compare the vacant trips of transferred vehicles in days when the transfer subsystem is active versus days transferring is not active.)

Figs. 10.b and 10.c depict the mean values of the GVCD for the reactive controller and the NMPC are 534 [m] and 475 [m]. Hence, the proactiveness of NMPC reduces the GVCD of the transferred vehicles by 12.4%. Moreover, using the reactive controller and the NMPC, 95% of the trips have GVCD less than 1094 [m] and 920 [m], respectively. This is equal to 13% improvements in reducing the matching distances without considering the effects of outliers. With no transferring, see Fig. 10.a, the standard deviation of the GVCD increases by 62.2%, which together with a large GVCD mean value indicate a considerable number of lengthy empty trips. In addition, the mean value of the GVCD with no transferring increases by 17.4% compared with the NMPC.

Fig. 11 illustrates the normalized histogram of the GVCD, whether the vehicle receives transferring command or not. It can be observed that the NMPC results in lower GVCD mean and standard deviation compared to no controller and the reactive controller. The mean values of the GVCD are 573 [m], 508 [m], and 491 [m] by using no controller, the reactive controller, and the NMPC, respectively. It shows 14.3% and 3.35% reduction of GVCD by using the NMPC compared to no controller and the reactive controller. These results demonstrate that, by following the transferring recommendations, the drivers reduce their total GVCD, which is their personal (selfish) gain. Accordingly, it can be expected that rational drivers would strategically follow the repositioning recommendations over time instead of random cruising during idle intervals.

5. Summary and future work

This article has proposed a model-based nonlinear model predictive controller (NMPC) to proactively reposition the idle vehicles in the network to balance the demand of waiting passengers and the supply of idle vehicles in ride-sourcing systems. The proposed

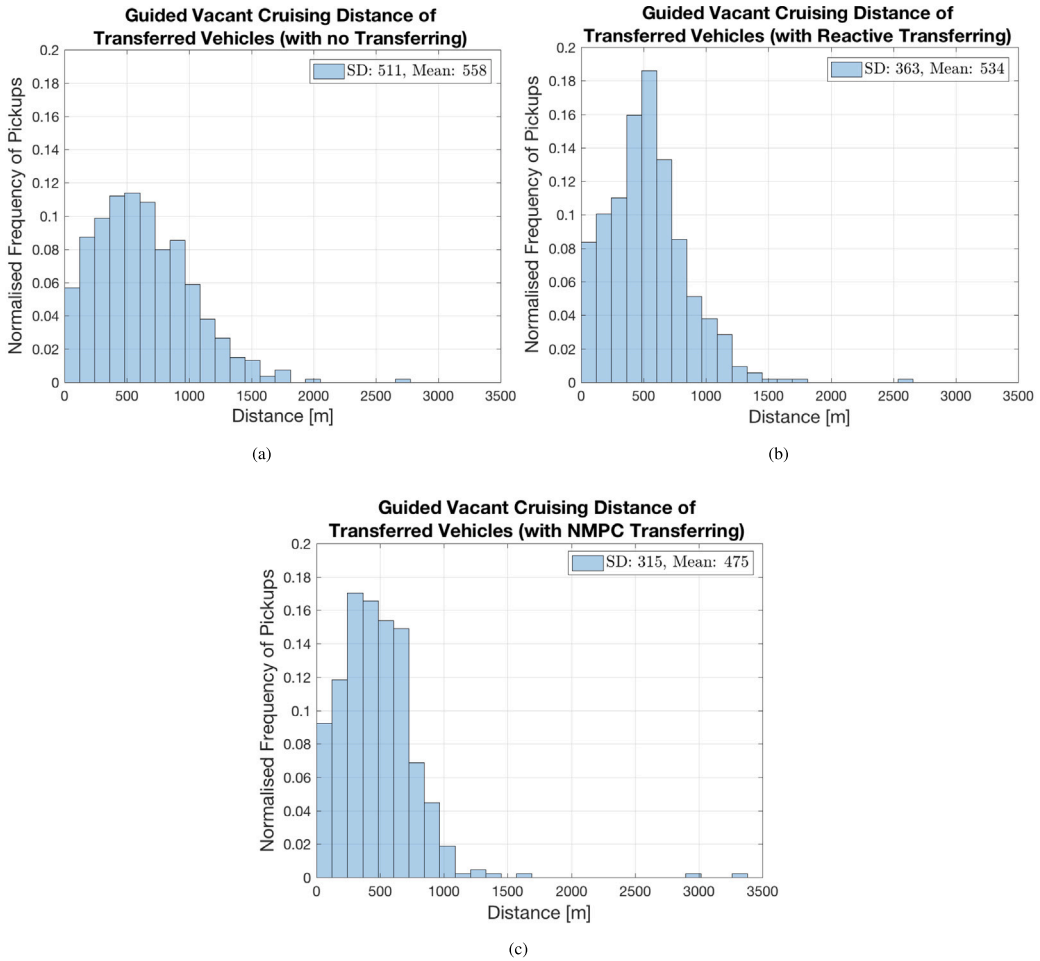

Fig. 10. Normalized histogram of GVCD for (a) the vehicles that at least have received a transferring command by the NMPC controller; however, they operate in no transfer control setting, (b) the vehicles that at least receive a transferring command by the reactive controller, and (c) the vehicles that at least receive a transferring command by the NMPC. Normalization refers to the conversion such that the sum of frequencies of all bins equals to 1.

NMPC is designed based on the model in Part I companion paper to reposition the vehicles to regions with a higher probability of being matched to passengers. To increase the controllability of the model and proactiveness of the transferring, closed-form formulations are suggested to estimate the rates of vehicle–passenger matchings during the prediction horizons. The NMPC utilizes the estimated values of the vehicle–passenger matchings and the model formulation in a state–space form to predict the evolution of the ride-sourcing vehicles (i.e., idle, transferred, dispatched, and occupied) and passengers (i.e., waiting and assigned). The NMPC determines the optimal transferring rates by solving a constrained finite-horizon optimal control problem to minimize the vehicles' and passengers' total unassigned time.

The effectiveness of the NMPC as the transferring method has been compared with no controller and a reactive controller using traffic microsimulation experiments. We have demonstrated that utilizing the proposed NMPC for repositioning idle vehicles improves the equality of the ride-sourcing system for both passengers and drivers. We showed that the NMPC has (i) increased the total number of served passengers by smaller fleet size, (ii) reduced the passengers' unassigned and waiting times, and (iii) reduced the vehicles' waiting times. In this study, we assumed drivers perform random cruising while in the idle state. Under this assumption, the results show that the NMPC helps reduce the cruising distance of vehicles and can incentivize drivers to follow transfer commands strategically. We would expect the results to hold even if the drivers park while idle. However, these results are still inconclusive that drivers will be more willing to follow the transfer commands instead of strategically cruising towards their self-identified hotspots. This compelling research priority requires explicitly modeling drivers' strategic search behaviors.

A future research direction is to consider the effect of transfer frequencies on (i) transferring rates, (ii) matching distances, and (iii) matching frequencies. Incorporating the transferring frequencies in modeling is a possible solution that results in a hybrid or a switching system in which the transfer frequencies can be obtained dynamically as a function of the evolution of the vehicles and passengers. Another challenging research is extending the proposed matching and transferring methods for ride-splitting and ride-sharing systems (Beojone and Geroliminis, 2021). In addition, transferring idle vehicles can be considered integrated with

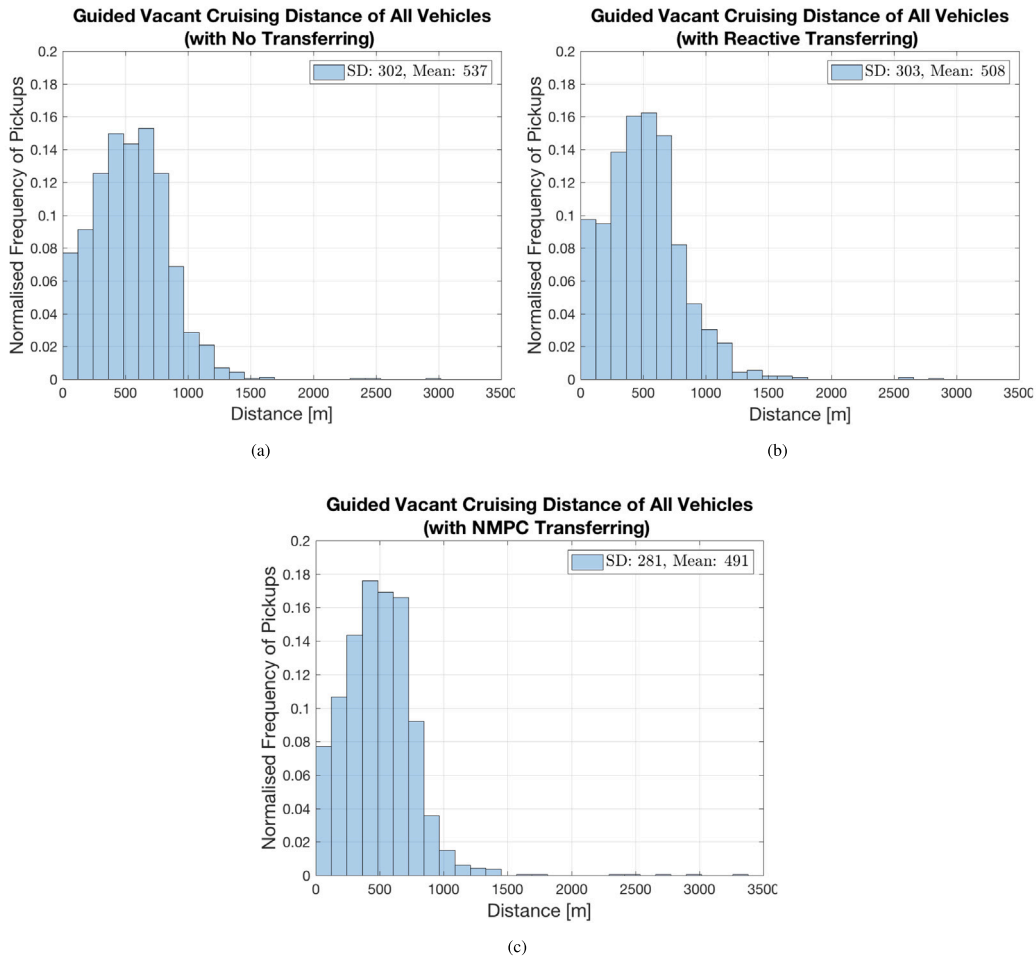

Fig. 11. Normalized histogram of GVCD for all the vehicles whether they receive the transferring command or not with (a) no controller, (b) the reactive controller, and (c) the NMPC. Normalization refers to the conversion such that the sum of frequencies of all bins equals to 1.

surge pricing methods to curb the supply–demand mismatch. In this paper, the arrival rate of waiting passengers is a time-varying exogenous factor. Considering the elasticity of this factor to repositioning, total delay, average passengers' unassigned time, and other long-term variables is a research priority. In addition, considering the supply characteristics (Ramezani et al., 2022) can be utilized for investigating detailed monetary incentivization of individual drivers and their compliance rate in following platform transferring recommendations. Furthermore, studying the effect of competition between multi-homing contractors on the supply of vehicles is another future research direction. Integration of ride-sourcing fleet information as probe vehicle data to estimate region-level traffic speed based on MFD and incorporating such traffic dynamics into the model and controller is also a research direction for further studies.

CRediT authorship contribution statement

Amir Hosein Valadkhani: Methodology, Software, Validation, Formal analysis, Investigation, Data curation, Writing – original draft. **Mohsen Ramezani:** Conceptualization, Methodology, Validation, Formal analysis, Investigation, Writing – original draft, Writing – review & editing, Supervision.

Acknowledgments

The authors thank the three anonymous reviewers for their valuable comments that improved the rigor and quality of the manuscript. This research was partially funded by the Australian Research Council (ARC) Discovery Early Career Researcher Award (DECRA) DE210100602.

Table A.3
The number of served passengers and operational fleet size for different settings of transfer subsystem using optimal myopic matching method with fixed matching interval of 30 [s] and no discarding. Averages of five microsimulation replications are reported. Numbers in parenthesis show percentage of the variation with respect to no transferring method.

	Average number of served passengers	Average Fleet Size	Average number of served passengers per vehicle
No transfer subsystem	1097	218	5.03
Reactive controller	1101 (0.4%)	212 (−1.8%)	5.19 (3.2%)
NMPC	1105 (0.7%)	212 (−1.8%)	5.21 (3.6%)

Table A.4
Unassigned and waiting delays with no controller, the reactive controller, and the NMPC using optimal myopic matching method with fixed matching interval of 30 [s] and no discarding. Results are obtained by averaging five microsimulation replications. Numbers in parenthesis show the percentage of variation with respect to the no transferring method.

	Passengers' unassigned time [s]		Passengers' waiting time [s]		Vehicles' unassigned time [s]		Vehicles' waiting time [s]	
	Mean	SD	Mean	SD	Mean	SD	Mean	SD
No transfer subsystem	40.4	54	197.0	137	148.0	329	793	1021
Reactive controller	39.5 (−2.2%)	51	192.2 (−2.4%)	134	153.0 (3.3%)	339	779 (−1.7%)	1009
NMPC	39.1 (−3.2%)	51	189.9 (−3.6%)	131	155.1 (4.8%)	337	777 (−2.0%)	1005

Appendix. Vehicle repositioning and matching without discarding

To isolate the effect of the proposed proactive transferring method from the proposed adaptive spatio-temporal matching in Part I paper, we employ the optimal myopic method with a fixed matching interval of 30 [s] and no discarding as the matching method. This would help us scrutinize the transferring method in isolation. Note that any transferring methods require a pool of idle vehicles that can be potentially transferred to balance the supply and demand in different parts of the network. Thus, a matching method such as optimal myopic that exhausts all the supply resources of idle vehicles for shorter passengers' matching times, at the expense of long-distance matchings, would do a disservice to any transferring method (i.e., reducing the number of idle vehicles reduces the effectiveness of the transferring method).

Table A.3 shows the effect of the transfer subsystem on the average number of served passengers and average fleet size. Table A.4 lists the performance of the three transferring settings on vehicles' and passengers' delays. As shown in Table A.3, repositioning mildly increases the average number of served passengers and reduces the fleet size that is required to serve the passengers. The reason is that the optimal myopic matching method consumes all the supply resources (i.e., idle vehicles). Comparing Table A.4 and Table 2, using optimal myopic with no discarding matching method instead of the proposed adaptive spatio-temporal method increases the passengers' and vehicles' unassigned times and waiting times. Furthermore, these results demonstrate that the optimal myopic matching method with no discarding reduces the performance of the transfer subsystem significantly.

References

Alonso-Mora, J., Samaranayake, S., Wallar, A., Frazzoli, E., Rus, D., 2017. On-demand high-capacity ride-sharing via dynamic trip-vehicle assignment. Proc. Natl. Acad. Sci. 114 (3), 462–467.

Barketau, M., Pesch, E., Shafransky, Y., 2015. Minimizing maximum weight of subsets of a maximum matching in a bipartite graph. Discrete Appl. Math. 196, 4–19.

Battifarano, M., Qian, Z.S., 2019. Predicting real-time surge pricing of ride-sourcing companies. Transp. Res. C 107, 444–462.

Beojone, C.V., Geroliminis, N., 2021. On the inefficiency of ride-sourcing services towards urban congestion. Transp. Res. C 124, 102890.

Braverman, A., Dai, J.G., Liu, X., Ying, L., 2019. Empty-car routing in ridesharing systems. Oper. Res. 67 (5), 1437–1452.

Byrd, R.H., Nocedal, J., Waltz, R.A., 2006. K nitro: An integrated package for nonlinear optimization. In: Large-Scale Nonlinear Optimization. Springer, pp. 35–59.

Chen, L., Valadkhani, A.H., Ramezani, M., 2021. Decentralised cooperative cruising of autonomous ride-sourcing fleets. Transp. Res. C 131, 103336.

Dandl, F., Hyland, M., Bogenberger, K., Mahmassani, H.S., 2019. Evaluating the impact of spatio-temporal demand forecast aggregation on the operational performance of shared autonomous mobility fleets. Transportation 46 (6), 1975–1996.

Haddad, J., Mirkin, B., 2021. Adaptive tracking of uncertain nonlinear systems under different types of input delays with urban traffic perimeter control application. Internat. J. Robust Nonlinear Control 31 (15), 6975–6990.

Illgen, S., Höck, M., 2019. Literature review of the vehicle relocation problem in one-way car sharing networks. Transp. Res. B 120, 193–204.

Jiao, G., Ramezani, M., 2022. Incentivizing shared rides in e-hailing markets: Dynamic discounting. Transp. Res. C 144, 103879.

Ke, J., Yang, H., Zheng, H., Chen, X., Jia, Y., Gong, P., Ye, J., 2018. Hexagon-based convolutional neural network for supply-demand forecasting of ride-sourcing services. IEEE Trans. Intell. Transp. Syst. 20 (11), 4160–4173.

Ke, J., Zheng, H., Yang, H., Chen, X.M., 2017. Short-term forecasting of passenger demand under on-demand ride services: A spatio-temporal deep learning approach. Transp. Res. C 85, 591–608.

Kouvelas, A., Saeedmanesh, M., Geroliminis, N., 2017. Enhancing model-based feedback perimeter control with data-driven online adaptive optimization. Transp. Res. B 96, 26–45.

Li, Y., Ramezani, M., 2022. Quasi revenue-neutral congestion pricing in cities: Crediting drivers to avoid city centers. Transp. Res. C 145, 103932.

Maciejewski, M., Bischoff, J., Nagel, K., 2016. An assignment-based approach to efficient real-time city-scale taxi dispatching. IEEE Intell. Syst. 31 (1), 68–77.

Narayanan, S., Chaniotakis, E., Antoniou, C., 2020. Shared autonomous vehicle services: A comprehensive review. Transp. Res. C 111, 255–293.
Nourinejad, M., Ramezani, M., 2019. Ride-sourcing modeling and pricing in non-equilibrium two-sided markets. Transp. Res. B.
Nourinejad, M., Zhu, S., Bahrami, S., Roorda, M.J., 2015. Vehicle relocation and staff rebalancing in one-way carsharing systems. Transp. Res. E 81, 98–113.
Pavone, M., Smith, S.L., Frazzoli, E., Rus, D., 2012. Robotic load balancing for mobility-on-demand systems. Int. J. Robot. Res. 31 (7), 839–854.
Ramezani, M., Nourinejad, M., 2018. Dynamic modeling and control of taxi services in large-scale urban networks: A macroscopic approach. Transp. Res. C 94, 203–219.
Ramezani, M., Yang, Y., Elmasry, J., Tang, P., 2022. An empirical study on characteristics of supply in e-hailing markets: a clustering approach. Transp. Lett. 1–14.
Sayarshad, H.R., Chow, J.Y., 2017. Non-myopic relocation of idle mobility-on-demand vehicles as a dynamic location-allocation-queueing problem. Transp. Res. E 106, 60–77.
Sirmatel, I.I., Geroliminis, N., 2021. Stabilization of city-scale road traffic networks via macroscopic fundamental diagram-based model predictive perimeter control. Control Eng. Pract. 109, 104750.
Vazifeh, M.M., Santi, P., Resta, G., Strogatz, S.H., Ratti, C., 2018. Addressing the minimum fleet problem in on-demand urban mobility. Nature 557 (7706), 534–538.
Wächter, A., Biegler, L.T., 2006. On the implementation of an interior-point filter line-search algorithm for large-scale nonlinear programming. Math. Program. 106 (1), 25–57.
Waltz, R.A., Morales, J.L., Nocedal, J., Orban, D., 2006. An interior algorithm for nonlinear optimization that combines line search and trust region steps. Math. Program. 107 (3), 391–408.
Wang, H., Yang, H., 2019. Ridesourcing systems: A framework and review. Transp. Res. B 129, 122–155.
Wu, X., Guo, J., Xian, K., Zhou, X., 2018. Hierarchical travel demand estimation using multiple data sources: A forward and backward propagation algorithmic framework on a layered computational graph. Transp. Res. C 96, 321–346.
Yang, H., Qin, X., Ke, J., Ye, J., 2020. Optimizing matching time interval and matching radius in on-demand ride-sourcing markets. Transp. Res. B 131, 84–105.
Yang, Y., Ramezani, M., 2023. A learning method for real-time repositioning in E-hailing services. IEEE Trans. Intell. Transp. Syst. 24 (2), 1644–1654.
Yildirimoglu, M., Sirmatel, I.I., Geroliminis, N., 2018. Hierarchical control of heterogeneous large-scale urban road networks via path assignment and regional route guidance. Transp. Res. B 118, 106–123.
Zha, L., Yin, Y., Du, Y., 2018a. Surge pricing and labor supply in the ride-sourcing market. Transp. Res. B 117, 708–722.
Zha, L., Yin, Y., Xu, Z., 2018b. Geometric matching and spatial pricing in ride-sourcing markets. Transp. Res. C 92, 58–75.
Zhang, R., Pavone, M., 2016. Control of robotic mobility-on-demand systems: a queueing-theoretical perspective. Int. J. Robot. Res. 35 (1–3), 186–203.
Zuniga-Garcia, N., Tec, M., Scott, J.G., Ruiz-Juri, N., Machemehl, R.B., 2020. Evaluation of ride-sourcing search frictions and driver productivity: A spatial denoising approach. Transp. Res. C 110, 346–367.